Chair for
Reliability Engineering

Maksym Besedin

Development of a Method for Assessing the Reliability of Machines Operating Under Stochastic Dynamic Loading

Master thesis

Folio: 01

Book: 02

Archive: 24

Nr. 006.01

2024

Development of a Method for Assessing the Reliability of Machines Operating Under Stochastic Dynamic Loading

To obtain an academic degree

Master of Science (Manufacturing Technology)

from the Faculty of Mechanical Engineering

at the Technical University of Dortmund

approved thesis

presented by

Maksym Besedin, B.Sc.

from

Sumy, Ukraine

Dortmund, 2024

Supervisor: Prof. Dr. Matthias G.R. Faes
Chair for Reliability Engineering
Technische Universität Dortmund

Co-Supervisor: Dr. Marcos Valdebenito
Chair for Reliability Engineering
Technische Universität Dortmund

Date of submission: 13 January 2025

Acknowledgement

With this acknowledgement I would like to express my sincere gratitude to Dr. Xuan-Yi Zhang for the great contribution to this master thesis. Dr. Xuan-Yi Zhang has always provided a thoughtful and constructive feedback based on her high level of expertise. Besides, it is hard to express how valuable was the guidance and support provided by Dr. Xuan-Yi Zhang throughout the whole process of completing this thesis and research in general.

I am especially thankful for the opportunity to cite the research paper of Dr. Xuan-Yi Zhang. This paper has served as a foundation for the development of the research on the scope of this thesis.

Preface

The MATLAB source codes for all the results presented in this thesis can be provided upon request to the author.

During the preparation of this thesis, the author utilized ChatGPT and other generative AI tools for rephrasing and restructuring the author's originally written text, as well as for checking grammar, punctuation, and language, all with the purpose of increasing readability. After using specific tool/service, the author reviewed and edited the content as needed and take full responsibility for the content of the publication.

Abstract

Reliability assessment of the structures plays a vital role in the design and construction phases as well as the lifetime of the system. For efficiency and lower computational costs, some real-world application systems are simplified using assumptions of linearity of the structure and/or Gaussianity of the applied loading. Reliability assessment, specifically first excursion probability evaluation, for the cases with such simplifications might be performed using various efficient methods that do not demand a large number of simulations and are therefore recognized to be efficient and accurate enough.

However, in some real-world applications, systems' responses are described as non-Gaussian, and some systems might have a non-linear behavior. In such cases, all the developed approaches for linear structures under Gaussian loadings cannot be applied anymore. Therefore, more general approaches should be applied, but these methods are known for high computational costs and lower efficiency.

In order to estimate the first excursion probability of linear systems under non-Gaussian loading, a new method has been developed. This method is based on the Importance Sampling procedure but at the same time also applies Gaussian approximation of the stochastic dynamic loading. Three different examples are presented for the validation of the developed method's accuracy and efficiency. Obtained results are compared with the results obtained by Monte Carlo Simulation. Non-Gaussian loading is modeled as Student's t distribution. One of the examples has a practical meaning for manufacturing and is related to the machining.

Table of contents

List of abbreviations

ALIS	Adaptive Linked Importance Sampling
CDF	Cumulative Distribution Function
COV	Coefficient of Variation
EIS	Efficient Importance Sampling
IS	Importance Sampling
ISD	Importance Sampling Density
ISURP	Importance Sampling Using Reference Points
MCS	Monte Carlo Simulation
MDOF	Multiple Degrees of Freedom
PDF	Probability Density Function
PF	Probability of Failure
SDOF	Single Degree of Freedom
SS	Subset Simulation
TDOF	Two Degrees of Freedom

List of figures

List of tables

1 Introduction

1.1 Motivation

In real-world engineering applications, the reliability of the structures and machines is critical for ensuring safe and performance-based design. This is the most relevant to fields such as construction, manufacturing, and the building industry, where the structural failures might appear due to stochastic and sometimes not predictable loading conditions. Estimation of the failure probability is a key approach to gain understanding of the system response under prescribed loading [1].

In the past years, research results have provided some efficient and accurate methods for the evaluation of failure probability of the linear systems under Gaussian loadings [2]. Such assumptions of system linearity or Gaussianity of the loading conditions provide a simplified model of real-world practical models, which make the evaluation of probabilities more efficient and easier [3]. However, in many realistic applications, the assumption about Gaussian loading may not hold, since observed structural responses are described as non-Gaussian. It leads to the conclusion that either external loading is non-Gaussian, or the structure has non-linearities, or both. These changes in the models bring more complexity, and consequently, methods valid for Gaussian loading may provide inaccurate results when applied to non-Gaussian loads [4]. As a result, engineers are forced to apply more general approaches, such as Monte Carlo Simulation (MCS) or Subset Simulation (SS), which stand out as a universally applicable methods capable of providing accurate solutions even for cases with non-linearity and non-Gaussianity [3, 5].

These limitations in reliability analysis highlight the demand for the new efficient and accurate approaches.

1.2 Objective

The main objective of this work is the development of a method for assessment of the reliability of structures subjected to uncertain loadings. This method takes Importance Sampling as a basis and applies Gaussian approximation to approach non-Gaussianity of the loading, while providing higher efficiency than the traditional methods such as Monte Carlo Simulation.

This work aims to present the applicability and efficiency of this method based on three practical examples, one of which demonstrates an industrial application in manufacturing. In addition, the accuracy of the method is going to be validated by comparing it with the results obtained using Monte Carlo Simulation.

2 State of the Art

The implementation of up-to-date methods for the evaluation of failure probabilities of the system plays an important role. New methods bring higher efficiency, time savings, and a wider range of applications. From the practical point of view, it means a longer lifetime of the structures and machines, and lower maintenance costs. This chapter provides an overview of the state of the art in the field of reliability assessment. Recent methods as well as basic approaches are reviewed in this section of the work. The efficiency of the mentioned methods, in addition to their applications, is discussed.

The chapter explains the purpose of the thesis by means of a literature review. Firstly, section 2.1 gives an overview of the recent approaches being used for the estimation of the failure probability of the linear systems under Gaussian loading. Section 2.2 discusses more general methods for applications involving non-linear systems and non-Gaussian loading, while also highlighting relevance of this thesis.

2.1 Failure probability of linear systems subjected to Gaussian loading

Linear systems are characterized by simplified relationships between the loading that is applied to the system and the response of the system [3]. Linearity helps to avoid the complexities introduced by nonlinear behavior, simplifying the problem significantly. At the same time, when the system is subjected to a loading that can be described as a Gaussian distribution, the system's output remains Gaussian [3]. This kind of distribution is mathematically elegant, since it is fully characterized by the mean and (co)variance.

In recent years, several approaches have been developed to evaluate the first excursion probability of the system. For instance, importance sampling techniques [6, 7, 8, 9] have been developed with the aim of shifting the distribution closer to the failure region, so as to produce more samples lying in the failure region and therefore increase the efficiency [3, 10]. The importance sampling approach is able to estimate small first excursion probabilities (e.g., 10^{-3} or less) while keeping the number of simulations of the dynamic response relatively small (e.g., a few hundreds) [2]. The main aspect of the method is the choice of the importance sampling density (ISD). In cases when the dimensionality of the problem is not too large and the region of failure is relatively simple to describe, several different schemes for constructing the importance sampling density, such as those based on design points [8, 11, 12, 13, 14, 15] or adaptive presamples [16, 17, 18, 19], are found to be applicable. The design points, or presamples, are usually obtained numerically by means of optimization or simulation with the integrand function being directly used. When it comes to large dimensions and the problem becomes more complex, however, it may be challenging to obtain sufficient knowledge in order to construct an apropriate importance sampling density [3, 10, 20]. This was proved in [21], showing that Importance Sampling (IS) does generally not work in high dimensions unless some very specific conditions are met. On the contrary, an algorithm referred to as Adaptive Linked Importance Sampling

(ALIS) has been introduced in [22]. The main idea of this algorithm is to replace the fixed importance sampling density used in conventional importance sampling with a family of intermediate distributions that gradually converge to the target optimal importance sampling density associated with the conditional probability given the failure event. The general formulation of adaptive linked importance sampling enables a wider choice of intermediate importance sampling densities. It has been demonstrated on examples that ALIS offers significant improvements over techniques such as Subset Simulation. Specifically, it has been shown that the choice of intermediate importance sampling densities prescribed by Subset Simulation may not be optimal. Numerical examples presented in the paper show the efficiency and accuracy of the proposed method [22].

In addition, [23] shows an Importance Sampling scheme that was deduced in an alternative manner using the concept of Domain Decomposition and enhanced by taking averages along a given sampling direction. At the same time, the application of Directional Importance Sampling has been investigated [24, 25]. This method has been used to determine small first excursion probabilities of linear structures subject to dynamic Gaussian loading [2].

2.2 Non-linear systems and non-Gaussian loading

As soon as the system is characterized as non-linear or the applied load as non-Gaussian, methods discussed in section 2.1 cannot be applied anymore. In this case, more general approaches and methods such as Monte Carlo and its more advanced variants [2, 26, 27] may be applied for the evaluation of the failure probability of the system. Monte Carlo Simulation [6, 28] is considered to be a reliable approach regardless of the type and dimension of the problem. The main disadvantage, however, is that this method is not efficient when dealing with small probabilities (e.g., $P_F \leq 10^{-3}$) because the amount of samples, and therefore the large scale of numerical models required to obtain a specified accuracy, is proportional to $1/P_F$. As a matter of fact, in order to find small probabilities, information from rare samples lying in the failure region is required. It means that in most cases many samples would be needed before a failure occurs [10].

To obtain higher efficiency while at the same time keeping the robustness of MCS to the dimensionality of the problem and the complexity of the failure region, another simulation method, called Subset Simulation has been developed. This method is used to evaluate small failure probabilities encountered in reliability analysis of engineering systems. The main idea of this method is to express the failure probability of the system as a product of larger conditional failure probabilities. This is achieved by introducing intermediate failure events. If the conditional events are chosen sufficiently, the conditional failure probabilities can be made large enough so that they may be estimated by means of simulation using a small number of samples. By applying this method, the problem of high calculational effort for the calculation of a small failure probability is now approached by calculation of a sequence of conditional probabilities, which can be estimated by means of simulation with a higher efficiency [10].

Obviously, there is a lack of efficient methods to deal with non-linear systems and non-Gaussian loads. This thesis focuses on the development of a new method for the assessment of the reliability of structures subjected to stochastic dynamic loading. To be more specific, this approach deals with non-Gaussian loading by means of Gaussian approximation, while giving

higher efficiency than conventional methods such as MCS. This work shows the application of a newly developed method to the reliability assessment of machines operating under prescribed loading, which has a practical meaning for manufacturing.

3 Theoretical Background

3.1 Problem formulation

This chapter provides an overview of the fundamental concepts relevant to the problems addressed in this work, with a particular focus on calculating the first excursion probability of a linear mechanical system subjected to non-Gaussian loading.

This section starts with the definition of the system structural model in sub-section 3.1.1. After the definition of the system model, system loading is defined in sub-section 3.1.2. Then in sub-section 3.1.3 response of a system is discussed, and sufficient formulations are presented. After the response formulation, sub-section 3.1.4 represents system failure under the loading.

3.1.1 System model

Let us take into account a linear model of a structural system, which is considered to be elastic and with classical damping. The structural system is considered to be under loading $p(t)$, which is assumed to be scalar. The equation of motion for the system [29, 30]:

$$\boldsymbol{M}\ddot{\boldsymbol{\eta}}(t) + \boldsymbol{C}\dot{\boldsymbol{\eta}}(t) + \boldsymbol{K}\boldsymbol{\eta}(t) = \boldsymbol{q}p(t) \tag{3-1}$$

where $\ddot{\boldsymbol{\eta}}(t)$, $\dot{\boldsymbol{\eta}}(t)$ and $\boldsymbol{\eta}(t)$ are vectors for acceleration, velocity, and displacement, respectively. Mentioned vectors have a dimension of $n_D \times 1$, where n_D stands for the number of degrees of freedom of the system. The modeled system is characterized by the mass matrix $\boldsymbol{M}$, (classical) damping matrix $\boldsymbol{C}$, and stiffness matrix $\boldsymbol{K}$ – all of dimension $n_D \times n_D$. Loading $p(t)$ and the corresponding degrees of freedom of the structure are coupled by means of a vector $\boldsymbol{q}$ of dimension $n_D \times 1$. The system is assumed to be initially at rest: $\boldsymbol{\eta}(0) = \dot{\boldsymbol{\eta}}(0) = 0$ [29].

3.1.2 System loading

The dynamic loading $p(t)$ is described as a discrete process whose discrete time realizations are collected in vector $\boldsymbol{p}$ of a duration T and dimension n_T, where n_T is the total number of time discretization steps over the duration T, so that $n_T = T/\Delta t + 1$, where Δt denotes the time step. In this work, $p(t)$ is modeled by non-Gaussian white noise. It means that $\boldsymbol{p}$ is also non-Gaussian. By means of the inverse-normal transformation, $\boldsymbol{p}$ can be expressed as [29]:

$$\boldsymbol{p} = F_p^{-1}[\Phi_{\boldsymbol{z}}(\boldsymbol{z})] \tag{3-2}$$

where $\boldsymbol{z}$ is a vector that consists of random standard Gaussian variables of a dimension $n_T \times 1$; $F_{\boldsymbol{p}}(\cdot)$ and $\Phi_{\boldsymbol{z}}(\cdot)$ are the cumulative distribution functions (CDFs) associated with $\boldsymbol{p}$ and $\boldsymbol{z}$, respectively.

3.1.3 System response

The response of interest of the system $x_i(t, \boldsymbol{p}), i = 1, \dots, n_x$, can be calculated through the convolution integral [29, 31]:

$$x_i(t, \boldsymbol{p}) = \int_0^t h_i(t-\tau)\, p(\tau) d\tau, i = 1, \dots, n_x \tag{3-3}$$

where $h_i(\cdot)$ represents the unit impulse response function of the ith response $x_i(t, \boldsymbol{p})$. For the case with multi degree of freedom system, where $x_i(t, \boldsymbol{p})$ is a linear combination of the displacement vector constituents, $h_i(\cdot)$ represented as [29]:

$$h_i(t) = \sum_{r=1}^{n_D} \frac{\boldsymbol{\gamma}_i^T \boldsymbol{\phi}_r \boldsymbol{\phi}_r^T \boldsymbol{q}}{\boldsymbol{\phi}_r^T \boldsymbol{M} \boldsymbol{\phi}_r} \frac{1}{\omega_{d,r}} e^{-\zeta_r \omega_r t} \sin\left(\omega_{d,r} t\right) \tag{3-4}$$

where $\boldsymbol{\gamma}_i$ is a constant vector; $\boldsymbol{\phi}_r$ is the eigenvector (mode shape) corresponding to the r-th mode; ω_r is the natural frequency of the r-th mode; ζ_r is the damping ratio of the r-th mode; and $\omega_{d,r} = \omega_r \sqrt{1-\zeta_r^2}$ is the r-th damped frequency. This representation of Eq. (3-4) only holds true for the underdamped case when the damping ratio is below 1 ($\zeta < 1$). For the overdamped cases when the damping ratio is larger than 1 ($\zeta > 1$), an equation for the impulse response function would look like [32]:

$$h_i(t) = \sum_{r=1}^{n_D} \frac{\boldsymbol{\gamma}_i^T \boldsymbol{\phi}_r \boldsymbol{\phi}_r^T \boldsymbol{q}}{\boldsymbol{\phi}_r^T \boldsymbol{M} \boldsymbol{\phi}_r} \frac{1}{2\omega_{n,r}\sqrt{\zeta^2-1}} \left(e^{-\omega_{n,r}\left(\zeta - \sqrt{\zeta^2-1}\right)t} - e^{-\omega_{n,r}\left(\zeta + \sqrt{\zeta^2-1}\right)t} \right) \tag{3-5}$$

For the critically damped case when the damping ratio is around 1 ($\zeta = 1$), the impulse response function would be expressed as follows [32]:

$$h_i(t) = \sum_{r=1}^{n_D} \frac{\boldsymbol{\gamma}_i^T \boldsymbol{\phi}_r \boldsymbol{\phi}_r^T \boldsymbol{q} t}{\boldsymbol{\phi}_r^T \boldsymbol{M} \boldsymbol{\phi}_r} e^{-\omega_{n,r} t} \tag{3-6}$$

Considering the discrete time representation, the response at the k-th time instant $x_i(t_k, \boldsymbol{p})$ is:

$$x_i(t_k, \boldsymbol{p}) = \sum_{l=1}^{k} \Delta t \epsilon_l h_i(t_k - t_l)\, p(t_l) = \boldsymbol{h}_i(t_k) \boldsymbol{p} \tag{3-7}$$

where $\boldsymbol{h}_i(t_k)$ is a vector of a dimension $1 \times n_T$, with the l-th element of $\boldsymbol{h}_i(t_k)$ equal to $\Delta t \epsilon_l h_i(t_k - t_l)$ for $l \leq k$ and 0 for $l > k$. In this work, ϵ_l is selected in accordance with the trapezoidal integration rule [33], stating $\epsilon_l = 1/2$ if $l = 1$ or $l = k$; and $\epsilon_l = 1$ otherwise. Considering the mentioned above, the response vector can be represented in a matrix form such as:

$$\boldsymbol{x}_i = \begin{Bmatrix} x_i(t_1) \\ x_i(t_2) \\ x_i(t_3) \\ \vdots \\ x_i(t_{n_T}) \end{Bmatrix} = \Delta t \begin{bmatrix} \epsilon_1 h_i(0) & 0 & 0 & 0 & \dots & 0 \\ \epsilon_1 h_i(\Delta t) & \epsilon_2 h_i(0) & 0 & 0 & \dots & 0 \\ \epsilon_1 h_i(2\Delta t) & \epsilon_2 h_i(\Delta t) & \epsilon_3 h_i(0) & 0 & \dots & 0 \\ \vdots & \vdots & \vdots & \vdots & \ddots & \vdots \\ \epsilon_1 h_i\left((n_T - 1)\Delta t\right) & \dots & \dots & \dots & \dots & \epsilon_{n_T} h_i(0) \end{bmatrix} \begin{Bmatrix} p(t_1) \\ p(t_2) \\ p(t_3) \\ \vdots \\ p(t_{n_T}) \end{Bmatrix} \tag{3-8}$$

The transformation matrix $\boldsymbol{A_i}$ might be called here, so that the response equation simplifies to the following form:

$$\boldsymbol{x}_i = \boldsymbol{A}_i \boldsymbol{p} \tag{3-9}$$

where $\boldsymbol{x}_i$ is a vector of dimension $n_T \times 1$, $\boldsymbol{A}_i$ is a matrix of dimension $n_T \times n_T$ and $\boldsymbol{p}$ is a vector of dimension $n_T \times 1$. Using Eq. (3-9), it is possible to establish a linear relationship between the load $\boldsymbol{p}$ and all the responses at all time instants, that is:

$$\boldsymbol{x} = \begin{Bmatrix} \boldsymbol{x}_1 \\ \vdots \\ \boldsymbol{x}_{n_x} \end{Bmatrix} = \begin{bmatrix} \boldsymbol{A}_1 \\ \vdots \\ \boldsymbol{A}_{n_x} \end{bmatrix} \boldsymbol{p} \tag{3-10}$$

3.1.4 System failure

The response of the system must not exceed the prescribed threshold in order to fulfill specific practical design requirements. An elementary failure event of the system at time instant t_k, which corresponds to the i-th response of interest, is denoted as $F_{i,k}$ and defined by the following expression [29]:

$$F_{i,k} = F_{i,k,1} \bigcup F_{i,k,2} \tag{3-11}$$

where $F_{i,k,1}$ and $F_{i,k,2}$ correspond to upper and lower excursion at time instant t_k for the i-th response of interest, respectively. Each of the upper and lower excursions are defined as follows [29]:

$$F_{i,k,1} = \{\boldsymbol{p} \in \Omega_{\boldsymbol{p}} : g_{i,1}(t_k, \boldsymbol{p}) \leq 0\}, \qquad F_{i,k,2} = \{\boldsymbol{p} \in \Omega_{\boldsymbol{p}} : g_{i,2}(t_k, \boldsymbol{p}) \leq 0\} \tag{3-12}$$

$$g_{i,1}(t_k, \boldsymbol{p}) = b_{i,1} - x_i(t_k, \boldsymbol{p}), \qquad g_{i,2}(t_k, \boldsymbol{p}) = x_i(t_k, \boldsymbol{p}) - b_{i,2} \tag{3-13}$$

where $g_{i,1}(t_k, \boldsymbol{p})$ and $g_{i,2}(t_k, \boldsymbol{p})$ are the performance functions for upper and lower excursions, respectively, at time instant t_k for the i-th response of interest. Thresholds for upper and lower excursions for the i-th response of interest are denoted as $b_{i,1}$ and $b_{i,2}$ respectively. Domain of the load $\boldsymbol{p}$ is noted as $\Omega_{\boldsymbol{p}}$ [29].

Failure of the structure over the time range [0, T], denoted as F, is defined as the union of elementary failure events $F_{i,k,s}$. Considering Eq. (3-11), failure of the structure is defined as [29]:

$$F = \bigcup_{i=1}^{n_x} \bigcup_{k=1}^{n_T} F_{i,k} = \bigcup_{i=1}^{n_x} \bigcup_{k=1}^{n_T} \bigcup_{s=1}^{2} F_{i,k,s} \tag{3-14}$$

3.2 Methodology

This chapter gives an explanation of some available methods used to solve the kind of problem that is approached in this work. Not only is the theoretical part explained, but also some algorithmic implementation details are discussed. First, Monte Carlo Simulation is presented in sub-section 3.2.1, where its application for the calculation of first excursion probability is explained as well. Then, sub-section 3.2.2 covers an approach based on Importance Sampling. After that, sub-section 3.2.3 introduces a more efficient approach denoted as Efficient Importance Sampling. Sub-section 3.2.4 presents an application of Importance Sampling using a Gaussian approximation for non-Gaussian loading, which is the main contribution of this thesis.

3.2.1 Monte Carlo Simulation

Practical implementation of the Monte Carlo method starts with the generation of the samples of the uncertain parameters in the standard normal space, which are:

$$\boldsymbol{z}^{(j)}, j = 1, 2, \dots, N \tag{3-15}$$

where $\boldsymbol{z}^{(j)}$ represents independently generated samples based on the probability density function $f_{\boldsymbol{z}}(\boldsymbol{z})$, which is represented in Figure 3-1. Number of samples is represented by N. The next step is to project samples into the physical space of uncertain variables using the transformation from Eq. (3-2). After that, for each of the samples in the physical space, a deterministic analysis is carried out, and the response(s) of interest are determined. Then, for each sample, system failure event is investigated following the performance function in Eq. (3-13), and the failure indicator function is defined as [34]:

$$I_F(\boldsymbol{z}) = \begin{cases} 1 & \text{if } \boldsymbol{z} \in F \\ 0 & \text{if } \boldsymbol{z} \notin F \end{cases} \tag{3-16}$$

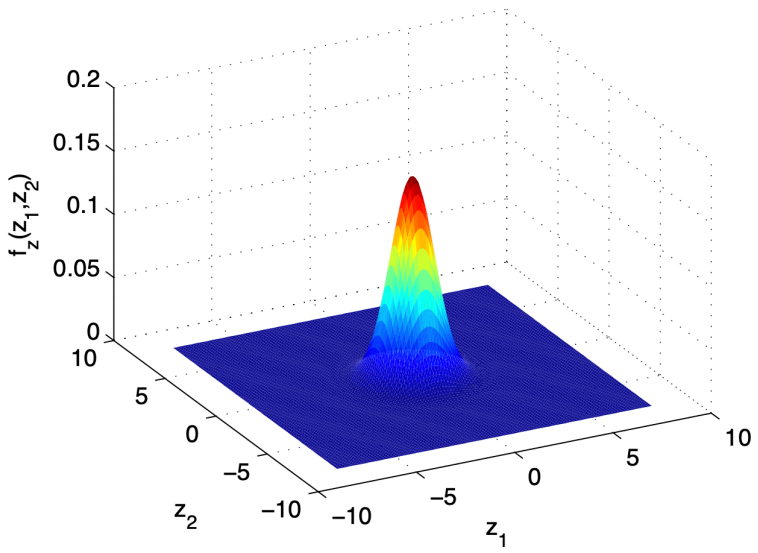

Figure 3-1: Probability density function of the normal distribution [34]

The failure probability of the system can be estimated as follows:

$$P[F] = \int_{\boldsymbol{z}\in R^2} I_F(\boldsymbol{z}) f_{\boldsymbol{Z}}(\boldsymbol{z}) d\boldsymbol{z} \approx \hat{P}[F] = \frac{1}{N}\sum_{j=1}^{N} I_F\left(\boldsymbol{z}^{(j)}\right) \quad \textbf{(3-17)}$$

where $\hat{P}[\cdot]$ represents an estimator of the failure probability $P[F]$. Therefore, there is an uncertainty about how close the estimator is to the real failure probability. One approach to determine this uncertainty is to calculate the coefficient of variation. The coefficient of variation associated with the Monte Carlo Method is calculated as follows [34]:

$$\delta_{MCS} = \sqrt{\frac{1-\hat{P}[F]}{N\hat{P}[F]}} \quad \textbf{(3-18)}$$

The estimator $\hat{P}[F]$ is considered to be reliable when $\delta_{MCS} < 10\%$. A reasonable estimator $\hat{P}[F]$ should have a coefficient of variation such that $\delta_{MCS} < 30\%$ [34].

3.2.2 Importance Sampling

The previously discussed Monte Carlo method is considered as a reliable approach and is used as a reference point for the results validation. On the contrary, it does not show high efficiency requiring a large number of samples in order to achieve stable results. This is due to the fact that the center of mass of the cloud of points (realizations of the vector of uncertain variables) associated with the Monte Carlo method is far away from the failure event, as shown in Figure 3-2 for an arbitrary two-dimensional performance function. One possible way to increase the frequency of failure samples generation is to shift the center of mass of the cloud of points towards the failure region, as shown in Figure 3-3. This approach has been named as Importance Sampling [8, 35].

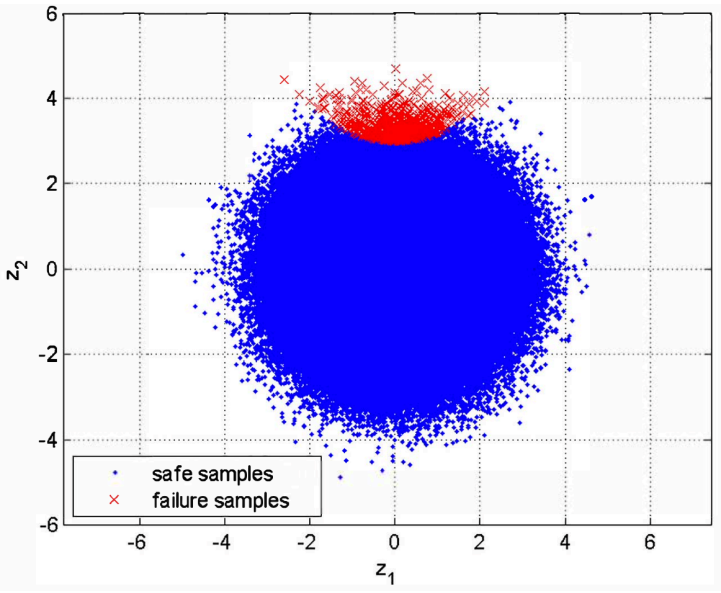

Figure 3-2: Realizations of the vector of uncertain variables associated with the Monte Carlo method [35]

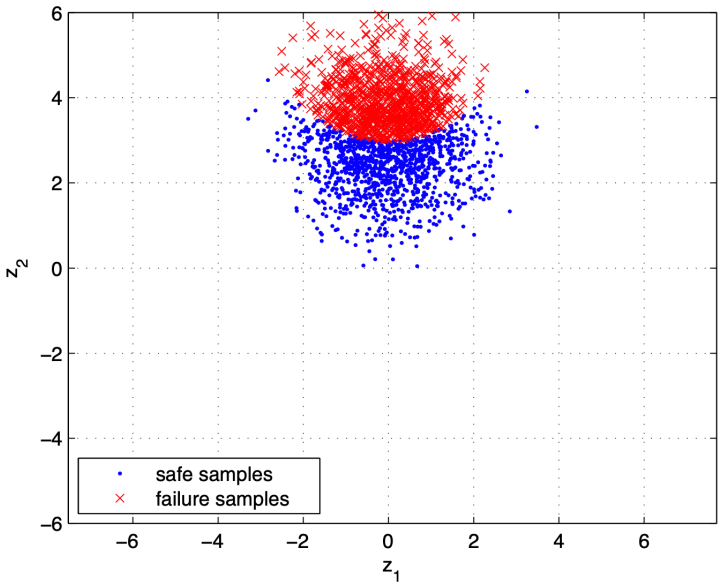

Figure 3-3: Realizations of the vector of uncertain variables associated with the Importance Sampling method [35]

In order to implement the Importance Sampling method, a probability density function $f_{IS,\boldsymbol{z}}(\boldsymbol{z})$ has to be considered. This function is called as Importance Sampling density function and has the following characteristics to take into account [35]:

- The function $f_{IS,\boldsymbol{z}}(\boldsymbol{z})$ is greater than zero throughout the failure domain.
- Most of the mass (or all of the mass) of the function $f_{IS,\boldsymbol{z}}(\boldsymbol{z})$ lies in the failure domain.
- The integral of $f_{IS,\boldsymbol{z}}(\boldsymbol{z})$ over the failure domain is close (or ideally equal) to 1.
- The probability density functions $f_{IS,\boldsymbol{z}}(\boldsymbol{z})$ and $f_{\boldsymbol{z}}(\boldsymbol{z})$ are similar to each other (proportional).

Practical implementation of the Importance Sampling method starts with the identification of the design point. The design point $\boldsymbol{z}^*$ is the realization of the vector $\boldsymbol{z}$ that belongs to the failure event and has the smallest Euclidean norm with respect to the origin. Alternatively, the design point $\boldsymbol{z}^*$ can be interpreted as the realization of the vector $\boldsymbol{z}$ that belongs to the failure event and that maximizes the value of the probability density function associated with $\boldsymbol{z}$. An example of a schematic representation of the design point $\boldsymbol{z}^*$ associated with a performance function (whose limit state function is linear) is illustrated in Figures 3-4 and 3-5 [35].

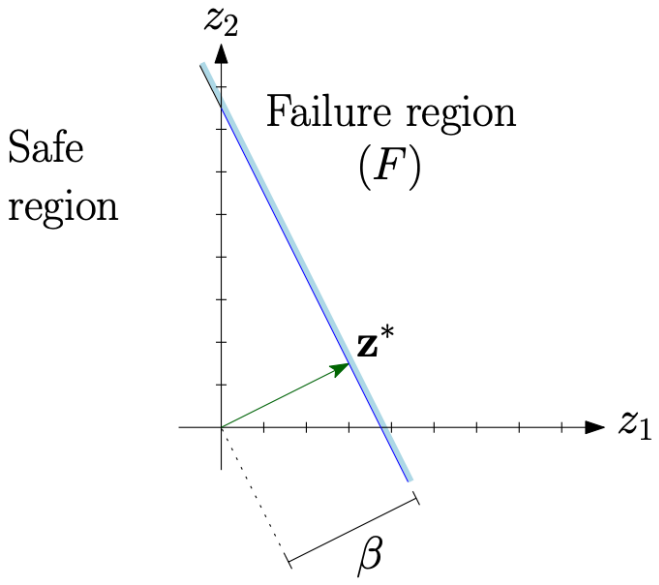

Figure 3-4: Example of schematic representation of the design point [35]

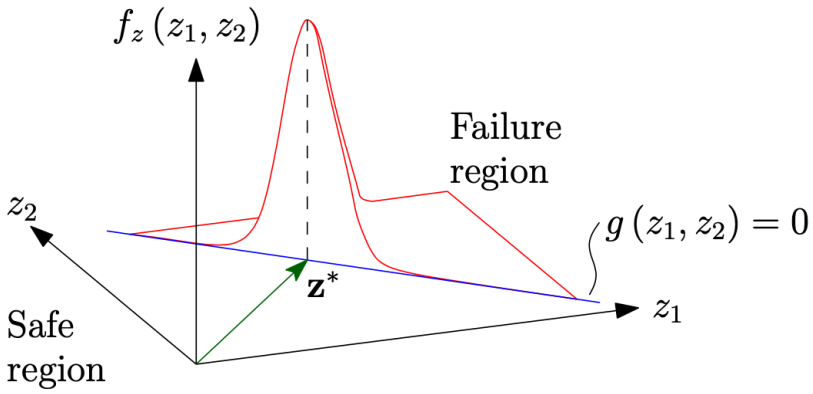

Figure 3-5: Example of schematic representation of the design point (isometric view) [35]

In order to determine the design point for a particular failure event, an optimization problem has to be solved:

$$\begin{aligned} &\min ||\mathbf{z}|| \\ &\text{subject to} \\ &g(\boldsymbol{z}) \leq 0 \end{aligned} \tag{3-19}$$

where $g(\boldsymbol{z})$ represents the performance function. In Eq. (3-19), $||\cdot||$ represents the Euclidean norm, which is also considered to be the reliability index and is denoted as β.

Before coming to the next step, an Importance Sampling probability density function $f_{IS,\boldsymbol{z}}(\boldsymbol{z})$ has to be defined. As can be seen from Figure 3-5, the neighborhood of the design point is the one that has the most impact on the probability integral, but this holds true only for a relatively small number of dimensions. Thus, the probability integral is re-defined as follows:

$$P[F] = \int_{g(\boldsymbol{z})\leq 0} \frac{f_{\boldsymbol{z}}(\boldsymbol{z})}{f_{IS,\boldsymbol{z}}(\boldsymbol{z})} f_{IS,\boldsymbol{z}}(\boldsymbol{z})\, d\boldsymbol{z} \tag{3-20}$$

Taking into account that the neighborhood of the design point in the standard normal space has the most impact on the probability integral, it makes sense to center the Importance Sampling probability density function at this point. Importance Sampling probability density function can be constructed in multiple ways. Nevertheless, a simple and effective way is to choose a normal distribution function centered at the design point with unit variance whose components are independent [21, 35]. In this case, the Importance Sampling probability density function has a distribution such that [36]:

$$f_{IS,\boldsymbol{z}}(\boldsymbol{z}) \sim N(\boldsymbol{\mu}, \sum) \tag{3-21}$$

where the symbol N denotes a multivariate normal distribution function, $\boldsymbol{\mu}$ is the expected value vector, and $\sum$ is the covariance matrix of the distribution, which are defined as follows:

$$\boldsymbol{\mu} = \boldsymbol{z}^* \tag{3-22}$$

$$\sum = \boldsymbol{I} = \begin{pmatrix} 1 & 0 & 0 & \cdots & 0 \\ 0 & 1 & 0 & \cdots & 0 \\ 0 & 0 & 1 & \cdots & 0 \\ \vdots & \vdots & \vdots & \ddots & \vdots \\ 0 & 0 & 0 & \cdots & 1 \end{pmatrix} \tag{3-23}$$

where $\boldsymbol{I}$ is the identity matrix.

When the problem involves n_p design points, initially n_p distribution functions associated with Importance Sampling are introduced that have the form defined in Eq. (3-21).

$$f_{IS,\boldsymbol{z}}^{(k)}(\boldsymbol{z}) \sim N(z_k^*, \boldsymbol{I}), k = 1, \ldots, n_p \tag{3-24}$$

However, it is necessary to remember that the Importance Sampling probability density function must integrate to one. Therefore, this function is considered to be constructed based on a weighted sum of the distributions shown in Eq. (3-24).

$$f_{IS,\boldsymbol{z}}(\boldsymbol{z}) = \omega_{IS}^{(1)} f_{IS,\boldsymbol{z}}^{(1)}(\boldsymbol{z}) + \cdots + \omega_{IS}^{(n_p)} f_{IS,\boldsymbol{z}}^{(n_p)}(\boldsymbol{z}) \tag{3-25}$$

This Importance Sampling probability density function presented in Eq. (3-25) is a superposition of several normal distributions with different expected values. In graphical representation and for the specific case where $n_p = 2$, the probability density function associated with the discussed Importance Sampling probability density function could have an appearance similar to that which is shown in Figure 3-6.

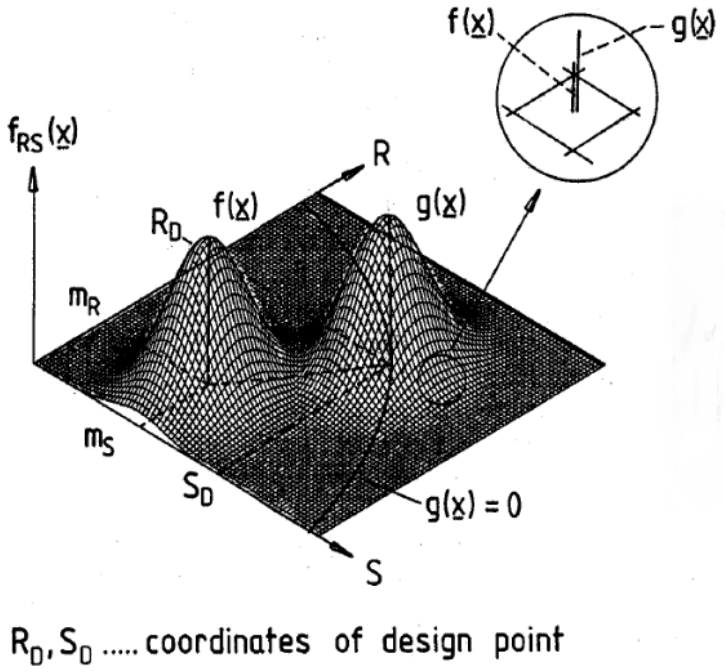

Figure 3-6: Graphical representation of possible appearance of the function $f_{IS,\boldsymbol{z}}(\boldsymbol{z})$ [8]

In Eq. (3-25), $\omega_{IS}^{(k)}, k = 1, \dots, n_p$ represents a weight with respect to the Importance Sampling probability density function, which is associated with each design point. The role of this weight $\omega_{IS}^{(k)}, k = 1, \dots, n_p$ is to ensure that the integral of the distribution function $f_{IS,\boldsymbol{z}}(\boldsymbol{z})$ is equal to 1 over the domain of the uncertain variables. Integrals of the Importance Sampling probability density functions associated with each design point $f_{IS,\boldsymbol{z}}^{(k)}(\boldsymbol{z}), k = 1, \dots, n_p$ separately are equal to 1 (since they are normal distribution functions). However, when added together, the integral will differ from 1. The weight $\omega_{IS}^{(k)}, k = 1, \dots, n_p$ has to fulfill the following conditions [36]:

$$\omega_{IS}^{(k)} \geq 0, k = 1, \dots, n_p \tag{3-26}$$

$$\sum_{k=1}^{n_p} \omega_{IS}^{(k)} = 1 \tag{3-27}$$

One possible way to choose the weight $\omega_{IS}^{(k)}, k = 1, \dots, n_p$ is to select it as being proportional to the probability associated with the reliability indices of each design point [8]:

$$\omega_{IS}^{(k)} = \frac{\Phi(-\beta_k)}{\sum_{k=1}^{n_p} \Phi(-\beta_k)}, k = 1, \dots, n_p \tag{3-28}$$

where $\Phi(\cdot)$ is the cumulative probability density function associated with the standard normal distribution. To generate samples of $\boldsymbol{z}$ distributed according to the Importance Sampling probability density function, it is necessary to consider the weights associated with each distribution. To be more specific, a random number u_1 has to be generated uniformly distributed between 0

and 1 ($u_1 \sim U[0,1]$) and the distribution associated with the q-th design point is selected such that it meets the following conditions [36]:

$$\omega_{IS}^{(1)} + \omega_{IS}^{(2)} + \cdots + \omega_{IS}^{(q-2)} + \omega_{IS}^{(q-1)} \leq u_1 \quad \textbf{(3-29)}$$

$$\omega_{IS}^{(1)} + \omega_{IS}^{(2)} + \cdots + \omega_{IS}^{(q-1)} + \omega_{IS}^{(q)} > u_1 \quad \textbf{(3-30)}$$

where q represents an integer less than or equal to the number of existing design points. Graphically, the number q can be represented as shown in Figure 3-7.

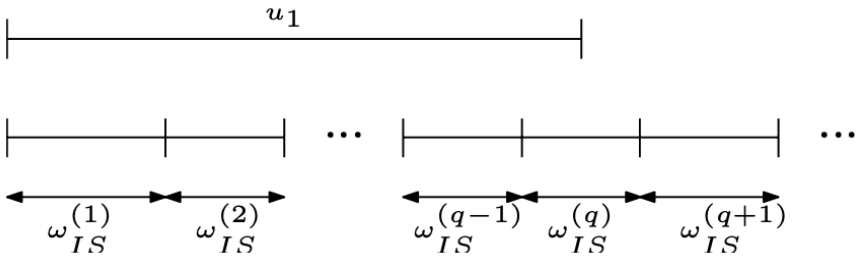

Figure 3-7: Graphical representation of the number q [36]

Once that a specific importance sampling density function has been selected, it is straightforward to generate one sample distributed according to that selected distribution. Then the whole procedure is repeated N times.

After that, a failure probability has to be estimated. The failure event can be expressed as [35]:

$$F = \{\boldsymbol{z} \in \mathbb{R}^{n_z} : g(\boldsymbol{z}) \leq 0\} \quad \textbf{(3-31)}$$

where n_z stands for the number of dimensions. Using Importance Sampling it can be defined as:

$$P[F] = \int_{\boldsymbol{z} \in \mathbb{R}^{n_z}} I_F(\boldsymbol{z}) f_{\boldsymbol{z}}(\boldsymbol{z})\, d\boldsymbol{z} \quad \textbf{(3-32)}$$

$$= \int_{\boldsymbol{z} \in \mathbb{R}^{n_z}} I_F(\boldsymbol{z}) \frac{f_{\boldsymbol{z}}(\boldsymbol{z})}{f_{IS,\boldsymbol{z}}(\boldsymbol{z})} f_{IS,\boldsymbol{z}}(\boldsymbol{z}) d\boldsymbol{z} \quad \textbf{(3-33)}$$

$$\approx \frac{1}{N} \sum_{j=1}^{N} I_F\left(\boldsymbol{z}^{(j)}\right) \frac{f_{\boldsymbol{z}}\left(\boldsymbol{z}^{(j)}\right)}{f_{IS,\boldsymbol{z}}\left(\boldsymbol{z}^{(j)}\right)}, \boldsymbol{z}^{(j)} \sim f_{IS,\boldsymbol{z}}(\boldsymbol{z}), j = 1, \ldots, N \quad \textbf{(3-34)}$$

Alternatively, the last equation can be expressed as follows:

$$P[F] \approx \hat{P}[F] = \frac{1}{N}\sum_{j=1}^{N} I_F\left(\boldsymbol{z}^{(j)}\right) w_{IS}\left(\boldsymbol{z}^{(j)}\right), \boldsymbol{z}^{(j)} \sim f_{IS,\boldsymbol{z}}(\boldsymbol{z}), j = 1, \dots, N \quad \textbf{(3-35)}$$

where $w_{IS}\left(\boldsymbol{z}^{(j)}\right)$ is the weight associated with the j-th sample of the uncertain parameters and is defined such as:

$$w_{IS}\left(\boldsymbol{z}^{(j)}\right) = \frac{f_{\boldsymbol{z}}\left(\boldsymbol{z}^{(j)}\right)}{f_{IS,\boldsymbol{z}}\left(\boldsymbol{z}^{(j)}\right)} \quad \textbf{(3-36)}$$

It is important to note that this weight $w_{IS}(\boldsymbol{z})$ has no relation to the weight $\omega_{IS}^{(k)}$ from Eq. (3-25). In addition, it is important to keep in mind that the above presented weight of a sample $w_{IS}(\cdot)$ is a scalar quantity that is equal to the joint probability density function of the standard normal variables divided by the Importance Sampling joint probability density function. From the last equations presented above, the main idea behind Importance Sampling becomes clear. The main idea is to generate samples of the vector $\boldsymbol{z}$ that are distributed with respect to the distribution function $f_{IS,\boldsymbol{z}}\left(\boldsymbol{z}^{(j)}\right)$. Following this procedure, failure samples are generated with a higher frequency. A weight function is included in the calculation of the failure estimator in Eq. (3-35) in order to weight the fact that the samples of $\boldsymbol{z}$ are not generated with respect to the original distribution. This weight function serves as a quotient between the original distribution function and the distribution function associated with Importance Sampling [35].

The probability density function associated with the original distribution can be expressed as follows:

$$f_{\boldsymbol{z}}(\boldsymbol{z}) = \frac{1}{\sqrt{|\boldsymbol{\Sigma}|}(2\pi)^{n_T/2}} e^{-\frac{1}{2}\left((\boldsymbol{z}-\boldsymbol{\mu})^T \boldsymbol{\Sigma}^{-1}(\boldsymbol{z}-\boldsymbol{\mu})\right)} \quad \textbf{(3-37)}$$

Considering Eq. (3-21), Eq. (3-22), and Eq. (3-23), the expression for the Importance Sampling probability density function is defined as:

$$f_{IS,\boldsymbol{z}}(\boldsymbol{z}) = \sum_{k=1}^{n_p} \omega_k f(\boldsymbol{z}, \boldsymbol{\mu}_k = \boldsymbol{z}_{\boldsymbol{k}}^*, \boldsymbol{I}) \quad \textbf{(3-38)}$$

$$= \sum_{k=1}^{n_p} \frac{\omega_k}{(2\pi)^{n_T/2}} e^{-\frac{1}{2}\left((\boldsymbol{z}-\boldsymbol{z}_k^*)^T \boldsymbol{I}(\boldsymbol{z}-\boldsymbol{z}_k^*)\right)} \quad \textbf{(3-39)}$$

Substituting Eq. (3-37) and Eq. (3-39) into Eq. (3-36) as well as considering that the Σ in this case is an identity matrix, the expression for the calculation of the weight $w_{IS}\left(\boldsymbol{z}^{(j)}\right)$ would be:

$$w_{IS}\left(\boldsymbol{z}^{(j)}\right) = \frac{\frac{1}{(2\pi)^{n_z}} e^{-\frac{1}{2}\boldsymbol{z}^{(j)^T}\boldsymbol{z}^{(j)}}}{\sum_{k=1}^{n_P} \frac{\omega_k}{(2\pi)^{n_z}} e^{-\frac{1}{2}\left(\left(\boldsymbol{z}^{(j)}-\boldsymbol{z}_k^*\right)^T \boldsymbol{I}\left(\boldsymbol{z}^{(j)}-\boldsymbol{z}_k^*\right)\right)}} \tag{3-40}$$

$$= \frac{e^{-\frac{1}{2}\boldsymbol{z}^{(j)^T}\boldsymbol{z}^{(j)}}}{\sum_{k=1}^{n_p} \omega_k \, e^{-\frac{1}{2}\left(\left(\boldsymbol{z}^{(j)}-\boldsymbol{z}_k^*\right)^T \boldsymbol{I}\left(\boldsymbol{z}^{(j)}-\boldsymbol{z}_k^*\right)\right)}} \tag{3-41}$$

Presented in Eq. (3-41) quotient $w_{IS}\left(\boldsymbol{z}^{(j)}\right)$ can be calculated directly in low-dimensional spaces. As soon as the analysis is performed in high-dimensional spaces, some significant numerical issues might arise due to properties of exponential functions in the numerator and denominator. In high dimensions, values inside the exponential terms might increase or decrease rapidly, which leads to overflowing (exponentials become too large) or underflowing (exponentials become too small).

In order to address these computational challenges, the whole expression for the calculation of the quotient from Eq. (3-41) can be simplified by taking the natural logarithm of $w_{IS}\left(\boldsymbol{z}^{(j)}\right)$. After implementation of the simplifying logarithm properties, the expression is exponentiated to return to the original form:

$$w_{IS}\left(\boldsymbol{z}^{(j)}\right) = exp\left(-\frac{1}{2}\boldsymbol{z}^{(j)^T}\boldsymbol{z}^{(j)} - \log\left(\sum_{k=1}^{n_p} \omega_k \, e^{-\frac{1}{2}\left(\left(\boldsymbol{z}^{(j)}-\boldsymbol{z}_k^*\right)^T \boldsymbol{I}\left(\boldsymbol{z}^{(j)}-\boldsymbol{z}_k^*\right)\right)}\right)\right) \tag{3-42}$$

Applying properties of the logarithm, products of exponential terms are converted into sums, which means less probability of overflowing or underflowing. Expression of Eq. (3-42) can be simplified even more by applying the definition of the Euclidean norm such that:

$$\boldsymbol{z}^{(j)^T}\boldsymbol{z}^{(j)} = \left\|\boldsymbol{z}^{(j)}\right\|^2 \tag{3-43}$$

Respectively:

$$\left(\boldsymbol{z}^{(j)} - \boldsymbol{z}_k^*\right)^T \boldsymbol{I}\left(\boldsymbol{z}^{(j)} - \boldsymbol{z}_k^*\right) = \left\|\boldsymbol{z}^{(j)} - \boldsymbol{z}_k^*\right\|^2 \tag{3-44}$$

Following, Eq. (3-42) would be:

$$w_{IS}\left(\boldsymbol{z}^{(j)}\right) = exp\left(-\frac{1}{2}\left\|\boldsymbol{z}^{(j)}\right\|^2 - \log\left(\sum_{k=1}^{n_p} \omega_k \, e^{-\frac{1}{2}\left\|\boldsymbol{z}^{(j)}-\boldsymbol{z}_k^*\right\|^2}\right)\right) \tag{3-45}$$

In Eq. (3-45), both exp and log are present, which might introduce some additional numerical instabilities when exponentiating large values or when taking the logarithm of small values.

Specifically, the logarithm of the summation of small values might cause some serious computational challenges. In order to address these challenges arising from taking logarithm of small values, a so-called "log-sum-exp" trick might be applied [37].

For the introduction of the "log-sum-exp" trick, let us take the following term from Eq. (3-45):

$$\log\left(\sum_{k=1}^{n_p}\omega_k\, e^{-\frac{1}{2}\left\|\boldsymbol{z}^{(j)}-\boldsymbol{z}_k^*\right\|^2}\right) \tag{3-46}$$

For the simplicity of the derivation, let us rewrite it as:

$$y=\log\left(\sum_{k=1}^{n_p}\exp\left(a_k\right)\right) \tag{3-47}$$

Solving the logarithm would give:

$$e^y=\sum_{k=1}^{n_p}\exp\left(a_k\right) \tag{3-48}$$

Introducing s as an arbitrary constant would give:

$$e^y=e^s\sum_{k=1}^{n_p}\exp\left(a_k-s\right) \tag{3-49}$$

Taking the logarithm to obtain y:

$$y=s+\log\sum_{k=1}^{n_p}\exp\left(a_k-s\right) \tag{3-50}$$

The biggest advantage of this approach is that the arbitrary constant s is shifting the values in the exponent while still giving the same result. Arbitrary constant s is set to be:

$$s=max\left\{a_1,\cdots,a_{n_p}\right\} \tag{3-51}$$

Applying this "log-sum-exp" trick into Eq. (3-45) would give the following expression:

$$w_{IS}\left(\boldsymbol{z}^{(j)}\right)=exp\left(-\frac{1}{2}\left\|\boldsymbol{z}^{(j)}\right\|^2-\left(s+\log\left(\sum_{k=1}^{n_p}\omega_k\, e^{-\frac{1}{2}\left\|\boldsymbol{z}^{(j)}-\boldsymbol{z}_k^*\right\|^2-s}\right)\right)\right) \tag{3-52}$$

Since this study focuses on the simulations in high dimensions, implementation of the discussed logarithmic simplification as well as "log-sum-exp" trick is essential in the scope of this work.

After the failure probability has been estimated, the uncertainty related to the Importance Sampling probability estimator can be defined by means of the coefficient of variation δ_{IS} [35]:

$$\delta_{IS} = \frac{\sqrt{V\left[\hat{P}[F]\right]}}{\hat{P}[F]} \tag{3-53}$$

$$\approx \frac{1}{\hat{P}[F]} \sqrt{\frac{1}{N(N-1)} \sum_{j=1}^{N} \left(I_F(\boldsymbol{z}^{(j)}) w_{IS}(\boldsymbol{z}^{(j)}) - \hat{P}[F]\right)^2} \tag{3-54}$$

where $V[\cdot]$ is the variance of the argument inside the square brackets.

3.2.3 Efficient Importance Sampling

In order to achieve greater efficiency, an alternative Importance Sampling probability density function might be designed. This new Importance Sampling probability density function is denoted as $f_{EIS,\boldsymbol{z}}(\boldsymbol{z})$, where EIS denotes Efficient Importance Sampling. However, it should be noted that EIS is only applicable whenever the performance function is linear with respect to Gaussian random variables. As this is not the case for the class of problems studied in this thesis, EIS is not applicable within the current study. Nevertheless, this technique is still presented in this thesis as it is a seminal work which has shed light on the development of many simulation schemes.

The whole procedure starts with the identification of the design points and reliability indices associated with the basic performance functions. Assuming linearity of these functions, the following formulas can be used [38, 39]:

$$\boldsymbol{z}_k^* = -g_k(\boldsymbol{0}) \frac{\nabla g_k(\boldsymbol{0})}{\|\nabla g_k(\boldsymbol{0})\|^2} \tag{3-55}$$

$$\beta_k = \frac{g_k(\boldsymbol{0})}{\|\nabla g_k(\boldsymbol{0})\|} \tag{3-56}$$

After the design points and reliability indices have been identified, the Efficient Importance Sampling Density Function has to be constructed. First of all, let us take a look at the probability of one failure domain. Let us consider the elemental performance functions $g_k(z), k = 1, \dots, n_p$. The elemental failure with respect to each of them is represented as follows [40]:

$$F_k = \{\boldsymbol{z} \in \mathbb{R}^{n_z} : g_k(\boldsymbol{z}) \leq 0\}, k = 1, \dots, n_p \tag{3-57}$$

Then, the failure event F is the union of the elementary failure events:

$$F = \bigcup_{k=1}^{n_p} F_k \tag{3-58}$$

The probability of occurrence of the basic failure event $P[F_k]$ can be estimated analytically (without the need for simulation techniques). In order to demonstrate this, take into account k-th performance function in Eq. (3-59) and assume that number of dimensions $n_z = 2$ for simplicity:

$$g_k(\boldsymbol{z}) = g_k(\mathbf{0}) + a_1^k z_1 + a_2^k z_2 \tag{3-59}$$

where a_1^k and a_2^k are constants and $g_k(\mathbf{0})$ stands for the performance function evaluated at the origin of the standard normal space. Then, the probability $P[F_k]$ is expressed as follows:

$$P[F_k] = P[g_k(\boldsymbol{z}) \leq 0] \tag{3-60}$$

$$= P\left[g_k(\mathbf{0}) + a_1^k z_1 + a_2^k z_2 \leq 0\right] \tag{3-61}$$

$$= P\left[a_1^k z_1 + a_2^k z_2 \leq -g_k(\mathbf{0})\right] \tag{3-62}$$

The expression $a_1^k z_1 + a_2^k z_2$ contains the sum of 2 independent normal distributions multiplied by a constant. Considering properties of the normal distribution, this sum is equal to another random variable z_S with expected value 0 and standard deviation $\sqrt{\left(a_1^k\right)^2 + \left(a_2^k\right)^2}$.

$$z_S \sim N(0, \left(a_1^k\right)^2 + \left(a_2^k\right)^2) \tag{3-63}$$

The mentioned random variable z_S can be represented by means of a standard normal variable z using the following equation:

$$z_S = z\sqrt{\left(a_1^k\right)^2 + \left(a_2^k\right)^2} \tag{3-64}$$

Substituting will give the following expression:

$$P[F_k] = P\left[z\sqrt{\left(a_1^k\right)^2 + \left(a_2^k\right)^2} \leq -g_k(\mathbf{0})\right] \tag{3-65}$$

$$= P\left[z \leq -\frac{g_k(\mathbf{0})}{\sqrt{\left(a_1^k\right)^2 + \left(a_2^k\right)^2}}\right] \tag{3-66}$$

Eq. (3-66) shows that in order to determine the probability, it is necessary to determine the probability that a standard normal random variable z is less than a certain number or equal to it. This

can be determined using the cumulative probability density function $\Phi(\cdot)$. Subsequently, the probability can be expressed as follows:

$$P[F_k] = \Phi\left(-\frac{g_k(\mathbf{0})}{\sqrt{\left(a_1^k\right)^2 + \left(a_2^k\right)^2}}\right) \tag{3-67}$$

It is important to remember that the term $g_k(\mathbf{0})/\sqrt{\left(a_1^k\right)^2 + \left(a_2^k\right)^2}$ represents the distance from the origin of the standard normal space to the limit state function associated with $g_k(\boldsymbol{z})$. Accordingly:

$$\beta_k = \frac{g_k(\mathbf{0})}{\sqrt{\left(a_1^k\right)^2 + \left(a_2^k\right)^2}} \tag{3-68}$$

$$P[F_k] = \Phi(-\beta_k) \tag{3-69}$$

The next step is to define a standard normal probability density function condition on one failure event. This function can be expressed using Bayes' theorem [40]:

$$f_z(\boldsymbol{z}|F_k) = \frac{P[\boldsymbol{z} \cap F_k]}{P[F_k]} = \frac{I_{F_k}(\boldsymbol{z}) f_{\boldsymbol{z}}(\boldsymbol{z})}{P[F_k]} \tag{3-70}$$

where $I_{F_k}(\boldsymbol{z})$ represents the indicator function associated with the failure event F_k. Considering also Eq. (3-69), the conditional probability density function can be expressed as follows:

$$f_z(\boldsymbol{z}|F_k) = \frac{I_{F_k}(\boldsymbol{z}) f_{\boldsymbol{z}}(\boldsymbol{z})}{\Phi(-\beta_k)} \tag{3-71}$$

This Eq. (3-71) can be interpreted as follows: from one side, it has a similar shape to a standard normal distribution, but from another point of view, it is truncated. The truncation is introduced through the indicator function $I_{F_k}(\boldsymbol{z})$. The constant $\Phi(-\beta_k)$ is used to ensure that the cumulative distribution function integrates to 1.

The efficient importance sampling density function is constructed using a weighted sum of the distributions in Eq. (3-71) [40].

$$f_{EIS,z}(\boldsymbol{z}) = \omega_{IS}^{(1)} f_z(\boldsymbol{z}|F_1) + \cdots + \omega_{IS}^{(n_p)} f_z\left(\boldsymbol{z}\middle|F_{n_p}\right) = \sum_{k=1}^{n_p} \omega_{IS}^{(k)} \frac{I_{F_k}(\boldsymbol{z}) f_{\boldsymbol{z}}(\boldsymbol{z})}{\Phi(-\beta_k)} \tag{3-72}$$

where $\omega_{IS}^{(k)}, k = 1, \dots, n_p$ is a weight that corresponds to the functions $f_z^{(k)}(\boldsymbol{z}|F_k), k = 1, \dots, n_p$ associated with each design point. This weight is selected proportional to the probability associated with the reliability indices of each design point as shown in Eq. (3-28) [40].

After that, in order to generate a samples from the importance sampling density function, one of the importance sampling density functions conditioned on a specific failure event F_k is chosen.

This is done following the procedure presented earlier for the importance sampling in Eq. (3-29) and Eq. (3-30). Once a density function associated with a particular design point is chosen, a sample distributed according to $f_z(\boldsymbol{z}|F_k)$ is generated. This procedure is quite particular and is described in the following. It starts with the generation of a sample of $\boldsymbol{z}^{(j)}$ distributed according to $f_{\boldsymbol{z}}(\boldsymbol{z})$. The next step is to subtract from the sample generated in the previous step the projection in the direction of the design point. It can be expressed mathematically as follows [38]:

$$\boldsymbol{z}_{\perp}^{(j)} = \boldsymbol{z}^{(j)} - (\boldsymbol{z}^{(j)} \cdot \boldsymbol{u}^*)\boldsymbol{u}^* \tag{3-73}$$

where $\boldsymbol{u}^*$ is the unit vector pointing in the direction of the design point and is calculated as:

$$\boldsymbol{u}^* = \frac{\boldsymbol{z}^*}{||\boldsymbol{z}^*||} \tag{3-74}$$

After the operation of subtraction, a sample $\boldsymbol{z}_{\parallel}^{(j)}$ has to be generated, which is parallel to the design point and is distributed according to a truncated normal distribution. This can be done following the next steps:

(a) Generate a number u, which is uniformly distributed between 0 and 1.

(b) Calculate a number α, which is distributed according to a truncated standard normal probability density function. This number α is calculated by the following formula:

$$\alpha = \Phi^{-1}(u + (1-u)\Phi(\beta)) \tag{3-75}$$

where $\Phi^{-1}(\cdot)$ represents the inverse standard normal cumulative density function.

(c) The sample $\boldsymbol{z}_{\parallel}^{(j)}$ is equal to:

$$\boldsymbol{z}_{\parallel}^{(j)} = \alpha \boldsymbol{u}^* \tag{3-76}$$

Finally, the resulting samples can be found as the sum of the samples in orthogonal and parallel directions to the design point.

$$\boldsymbol{z}_F^{(j)} = \boldsymbol{z}_{\perp}^{(j)} + \boldsymbol{z}_{\parallel}^{(j)} \tag{3-77}$$

The described procedure is illustrated schematically in Figure 3-8 for the case $n_z = 2$.

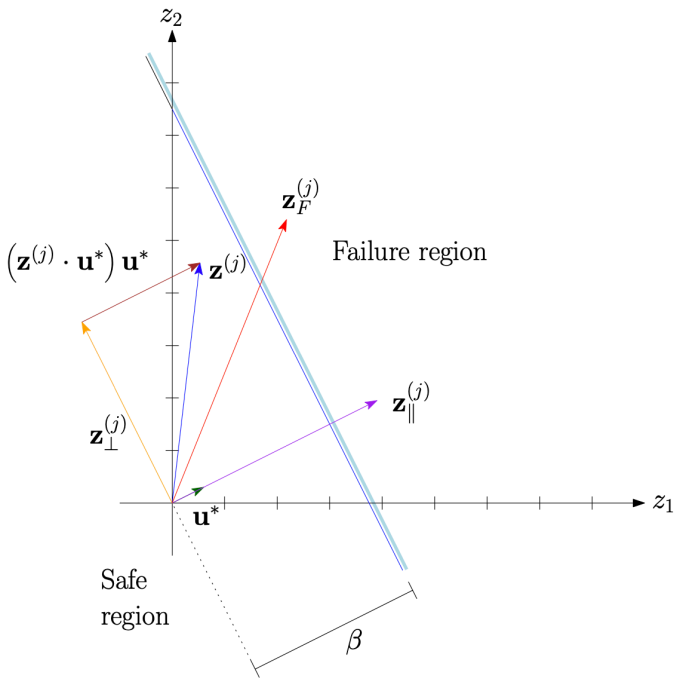

Figure 3-8: Schematic illustration of the described procedure for generating samples $z_F \sim f_z(z \mid F)$ [38]

Taking into account Eq. (3-35), Eq. (3-36), and Eq. (3-72), the estimator of the failure probability is defined as [40]:

$$P[F] \approx \hat{P}[F] = \frac{1}{N}\sum_{j=1}^{N} I_F\left(\mathbf{z}^{(j)}\right)\frac{f_{\mathbf{z}}\left(\mathbf{z}^{(j)}\right)}{f_{EIS,\mathbf{z}}\left(\mathbf{z}^{(j)}\right)}, \mathbf{z}^{(j)} \sim f_{EIS,\mathbf{z}}(\mathbf{z}) \tag{3-78}$$

The main advantage of the Efficient Importance Sampling probability density function $f_{EIS,\mathbf{z}}(\mathbf{z})$ over the Importance Sampling density function using design points $f_{IS,\mathbf{z}}(\mathbf{z})$ is that it is defined exclusively over the failure domain, as shown in Figure 3-9. It means that all generated samples fall within the failure domain such that $I_F(\mathbf{z}) = 1$. Then [40]:

$$\hat{P}[F] = \frac{1}{N}\sum_{j=1}^{N}\frac{f_{\mathbf{z}}\left(\mathbf{z}^{(j)}\right)}{\sum_{k=1}^{n_p}\omega_{IS}^{(k)}\frac{I_{F_k}(\mathbf{z}^{(j)})f_{\mathbf{z}}(\mathbf{z}^{(j)})}{\Phi(-\beta_k)}} \tag{3-79}$$

$$= \frac{1}{N}\sum_{j=1}^{N}\frac{f_{\mathbf{z}}\left(\mathbf{z}^{(j)}\right)}{\sum_{k=1}^{n_p}\frac{\Phi(-\beta_k)}{\sum_{k=1}^{n_p}\Phi(-\beta_k)}\frac{I_{F_k}(\mathbf{z}^{(j)})f_{\mathbf{z}}(\mathbf{z}^{(j)})}{\Phi(-\beta_k)}} \tag{3-80}$$

$$= \frac{1}{N}\sum_{j=1}^{N}\frac{\left(\sum_{k=1}^{n_p}\Phi(-\beta_k)\right)}{\sum_{k=1}^{n_p}I_{F_k}(\mathbf{z}^{(j)})} \tag{3-81}$$

If it is defined:

$$\hat{P}_F = \sum_{k=1}^{n_p} \Phi(-\beta_k) \tag{3-82}$$

the estimator of the failure probability is reduced to:

$$\hat{P}[F] = \frac{1}{N} \sum_{j=1}^{N} \frac{\hat{P}_F}{\sum_{k=1}^{n_p} I_{F_k}(\boldsymbol{z}^{(j)})} \tag{3-83}$$

The coefficient of variation is calculated as:

$$\delta_{EIS} = \frac{1}{\hat{P}[F]} \sqrt{\frac{1}{N(N-1)} \sum_{j=1}^{N} \left(\frac{\hat{P}_F}{\sum_{k=1}^{n_p} I_{F_k}(\boldsymbol{z}^{(j)})} - \hat{P}[F] \right)^2} \tag{3-84}$$

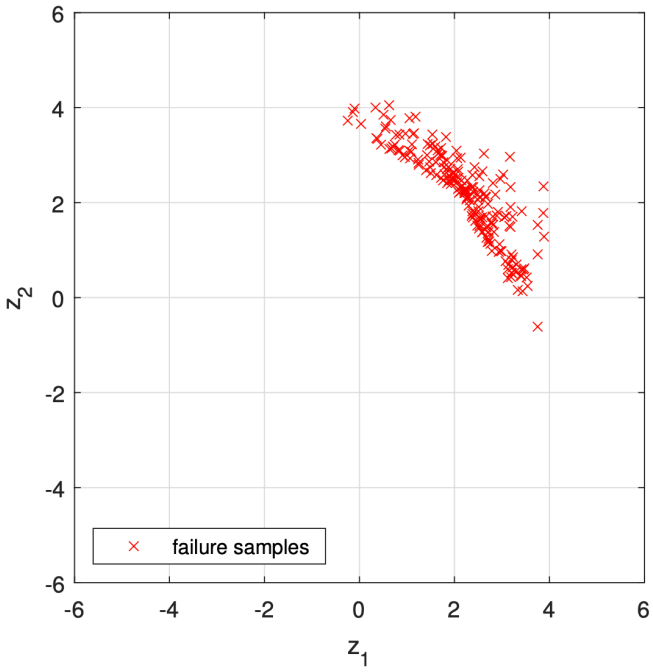

Figure 3-9: Realizations of the vector of uncertain variables associated with the Efficient Importance Sampling method [40]

In principle, EIS as presented in this Section 3.2.3 seems to be much more convenient that importance sampling using design points as shown in Section 3.2.2. The later holds true whenever the performance functions involved are linear with respect to the standard normal random variables $\boldsymbol{z}$. However, such assumption does not hold in this thesis, as it is considered that the loading $\boldsymbol{p}$ follows a non-Gaussian discrete white noise model, as discussed in detail in Eq. (3-2).

3.2.4 Importance Sampling for non-Gaussian loading

Boundary of the failure domain is defined by means of the limit state functions. In the reliability analysis of linear systems under Gaussian loading, limit state functions are linear. On the contrary, this thesis concentrates on the non-Gaussian loading, which is described in sub-section 3.1.2 and specifically in Eq. (3-2), where loading $\boldsymbol{p}$ is non-linear with respect to $\boldsymbol{z}$. Therefore, taking into account Eq. (3-9), response of the system $\boldsymbol{x}$ can be described as non-Gaussian. Thus, limit state functions are no longer linear as can be seen from Fig. 3-10.

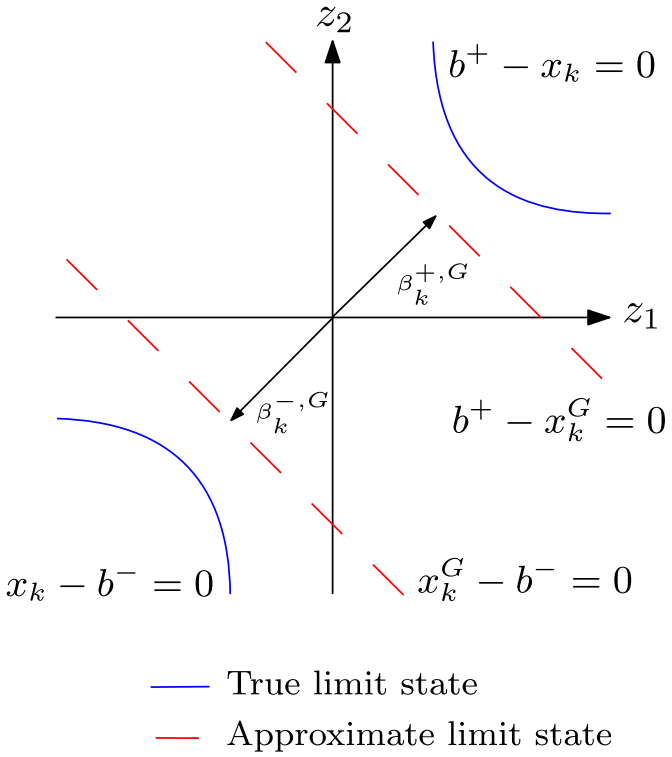

Figure 3-10: Graphical representation of the true limit states and approximate limit states

Since, the limit state functions are no longer linear, Efficient Importance Sampling cannot be applied, but Importance Sampling using design points is still applicable. It is important to note that finding design points by solving an optimization problem from Eq. (3-19) in high-dimensional spaces and non-linear performance functions is challenging. Therefore, applying Importance Sampling for non-Gaussian loading, instead of finding design points, a so-called “reference points” are defined. Reference points do not represent precisely design points, but sampling density can be still centered around them as graphically shown in Fig. 3-11.

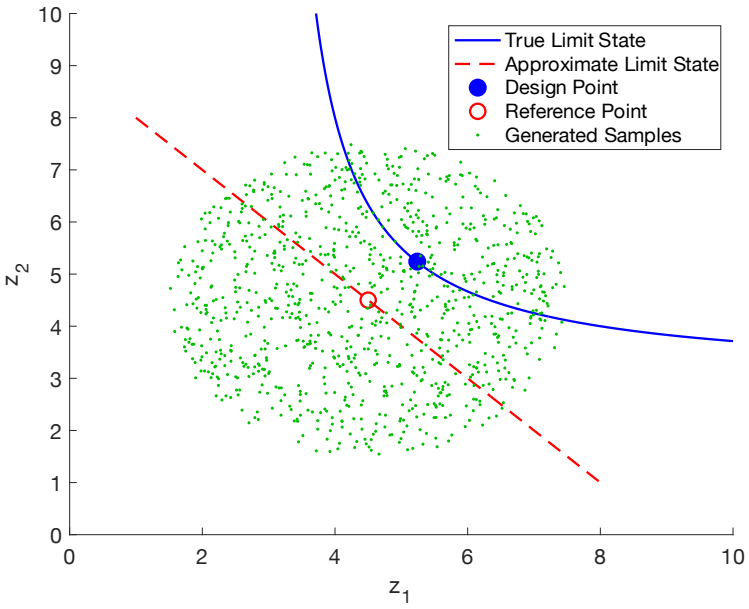

Figure 3-11: Graphical representation of the sampling density around reference point

In order to define reference points, non-Gaussian loading applied to the system needs to be Gaussianised. It means that the mean and standard deviation values of the original non-Gaussian loading and Gaussianised loading need to be as close to each other as possible. Such a matching between original non-Gaussian loading and Gaussianised loading can be seen in Fig. 3-12 and 3-13. These figures represent a visual examples of the probability density functions of non-Gaussian and Gaussian distributions, which might help to understand the approximation. Figure 3-12 depicts the PDF of a log-normal random variable and its Gaussianised counterpart, that is, a Gaussian variable with mean and variance identical to those of the log-normal random variable. Figure 3-13 is similar, except that it refers to a random variable following a Student's t distribution.

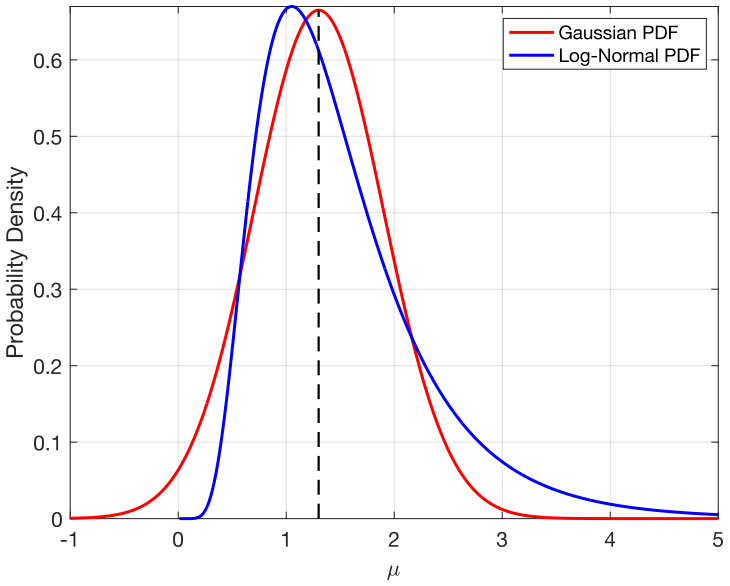

Figure 3-12: Probability Density Function (PDF) of log-normal and Gaussian distributions

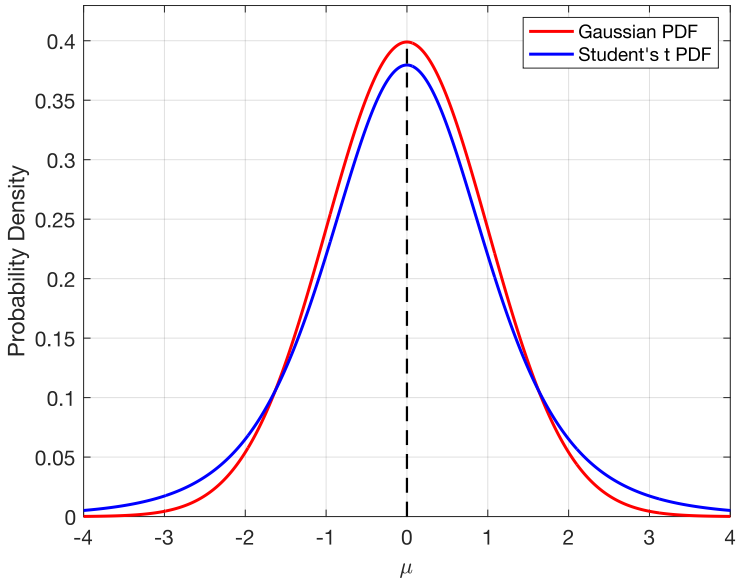

Figure 3-13: PDF of Student's t and Gaussian distributions

Performing an approximation, the non-Gaussian loading is now expressed in terms of a Gaussianised equivalent load, such as:

$$\boldsymbol{p}^G = \boldsymbol{\mu} + \boldsymbol{\sigma}_{st.dev.}\boldsymbol{z} \tag{3-85}$$

where $\boldsymbol{\mu}$ and $\boldsymbol{\sigma}_{st.dev.}$ are the mean vector and standard deviation matrix (which is a diagonal matrix due to the assumption of non-Gaussian white noise) of the non-Gaussian loading. If the loading is Gaussianised, the displacement of the system is also described as Gaussianised and can be expressed as follows:

$$\boldsymbol{x}_i^G = \boldsymbol{A}_i\boldsymbol{p}^G \tag{3-86}$$

$$= \boldsymbol{A}_i(\boldsymbol{\mu} + \boldsymbol{\sigma}_{st.dev.}\boldsymbol{z}) \tag{3-87}$$

$$= \boldsymbol{c}_i + \boldsymbol{D}_i\boldsymbol{z} \tag{3-88}$$

Graphical representation of Gaussianisation of the original non-Gaussian response is shown in Fig. 3-14. As observed from the Figure, the Gaussianised response is expected to approximate the non-Gaussian response. The quality of such approximation depends on how non-Gaussian the loading is.

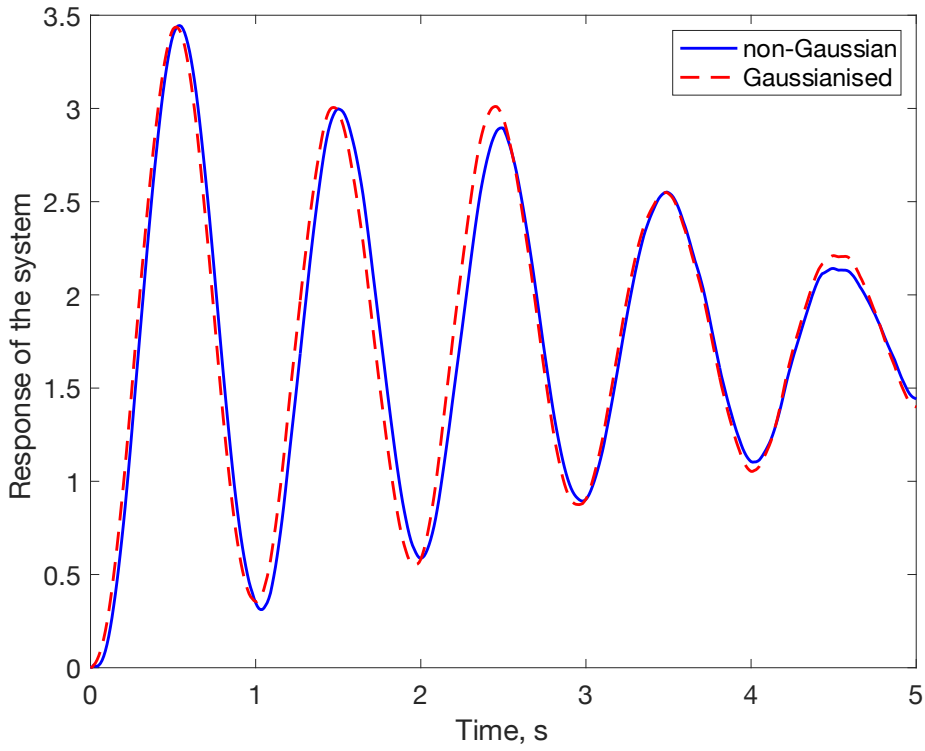

Figure 3-14: Graphical representation of Gaussianisation of the original non-Gaussian response

Taking Eq. (3-13) and Gaussianised displacement of the structure, performance functions for upper and lower excursions, respectively, at time instant t_k for the i-th response of interest are:

$$g_{i,1}^{G}(t_k, \boldsymbol{p}^G) = b_{i,1} - x_i^G(t_k, \boldsymbol{p}^G), \qquad g_{i,2}^{G}(t_k, \boldsymbol{p}^G) = x_i^G(t_k, \boldsymbol{p}^G) - b_{i,2} \tag{3-89}$$

Then, the reference points $\boldsymbol{z}_k^{*G}$ are defined with respect to Eq. (3-55) using the following formula:

$$\boldsymbol{z}_k^{*G} = -g_k^G(\boldsymbol{0}) \frac{\nabla g_k^G(\boldsymbol{0})}{\left\| \nabla g_k^G(\boldsymbol{0}) \right\|^2} \tag{3-90}$$

Considering Gaussianisation of the loading, the Importance Sampling probability density functions from Eq. (3-24) now has a distribution such that:

$$f_{IS,\boldsymbol{z}}^{(k),G}(\boldsymbol{z}) \sim N\left(\boldsymbol{z}_k^{*G}, \boldsymbol{I}\right), k = 1, \dots, n_p \tag{3-91}$$

Respectively, weighted sum of the distributions from Eq. (3-91) is:

$$f_{IS,\boldsymbol{z}}^{G}(\boldsymbol{z}) = \omega_{IS}^{(1),G} f_{IS,\boldsymbol{z}}^{(1),G}(\boldsymbol{z}) + \cdots + \omega_{IS}^{(n_p),G} f_{IS,\boldsymbol{z}}^{(n_p),G}(\boldsymbol{z}) \tag{3-92}$$

where the weight $\omega_{IS}^{(k),G}$ with respect to Eq. (3-28) is now defined as:

$$\omega_{IS}^{(k),G} = \frac{\Phi(-\beta_k^G)}{\sum_{k=1}^{n_p}\Phi(-\beta_k^G)}, k = 1, \dots, n_p \tag{3-93}$$

where β_k^G is the Euclidean norm of the reference point. Presented in Eq. (3-93) reliability indices are now defined using the following expression with respect to Eq. (3-56):

$$\beta_k^G = \frac{g_k^G(\mathbf{0})}{\left\|\nabla g_k^G(\mathbf{0})\right\|} \tag{3-94}$$

Referring to the Eq. (3-35), the failure probability can be estimated as:

$$P[F]^G \approx \hat{P}[F]^G = \frac{1}{N}\sum_{j=1}^{N} I_F\left(\boldsymbol{z}^{(j)}\right) w_{IS}^G\left(\boldsymbol{z}^{(j)}\right), \boldsymbol{z}^{(j)} \sim f_{IS,\boldsymbol{z}}^G(\boldsymbol{z}), j = 1, \dots, N \tag{3-95}$$

where the quotient $w_{IS}^G\left(\boldsymbol{z}^{(j)}\right)$ is now expressed with respect to Eq. (3-36) as:

$$w_{IS}^G\left(\boldsymbol{z}^{(j)}\right) = \frac{f_{\boldsymbol{z}}\left(\boldsymbol{z}^{(j)}\right)}{f_{IS,\boldsymbol{z}}^G(\boldsymbol{z}^{(j)})} \tag{3-96}$$

Taking into account Eq. (3-37) – Eq. (3-52), the weight $w_{IS}^G\left(\boldsymbol{z}^{(j)}\right)$ can be expressed as:

$$w_{IS}^G\left(\boldsymbol{z}^{(j)}\right) = exp\left(-\frac{1}{2}\left\|\boldsymbol{z}^{(j)}\right\|^2 - \left(s + \log\left(\sum_{k=1}^{n_p}\omega_k^G\, e^{-\frac{1}{2}\left\|\boldsymbol{z}^{(j)} - \boldsymbol{z}_k^{*G}\right\|^2 - s}\right)\right)\right) \tag{3-97}$$

Coefficient of variation from Eq. (3-54) is now defined as:

$$\delta_{IS}^G \approx \frac{1}{\hat{P}[F]^G}\sqrt{\frac{1}{N(N-1)}\sum_{j=1}^{N}\left(I_F(\boldsymbol{z}^{(j)}) w_{IS}^G(\boldsymbol{z}^{(j)}) - \hat{P}[F]\right)^2} \tag{3-98}$$

4 Practical Examples

Practical implementation of the theoretical background and methodologies discussed in the previous chapter is represented in this chapter by means of practical examples. Presented examples include a case with a single degree of freedom system (SDOF), a case with a two degrees of freedom system (TDOF), and a case with a multiple degrees of freedom system (MDOF). These examples are used in order to show the efficiency and accuracy of the developed method. All the reliability problems in this chapter are solved by means of implementation a newly developed Importance Sampling Using Reference Points (ISURP).

4.1 Single degree of freedom (SDOF) system

For the first example, a one-story shear beam model is taken [29], which is subjected to a non-Gaussian white noise following a Student's t distributed force (Figure 4-1). The considered system has a mass $m = 1kg$, stiffness $k = 4\pi^2 N/m$, and a classical damping ratio $d = 2\%$. Displacement of the beam related to the ground is taken as a response of interest. The force applied to the system is modeled as Student's t distribution with the spectral intensity $S = 1m^2/s^3$, duration $T = 15s$, and a discrete time step $\Delta t = 0.01s$, that corresponds to the spectral density $2\pi S/\Delta t$. Applied force is characterized by a mean value $\mu = 70$ and a standard deviation $\sigma_{std.dev.} = \sqrt{2\pi S/\Delta t}$. Estimation of the first excursion probability of the system is considered to be the main objective.

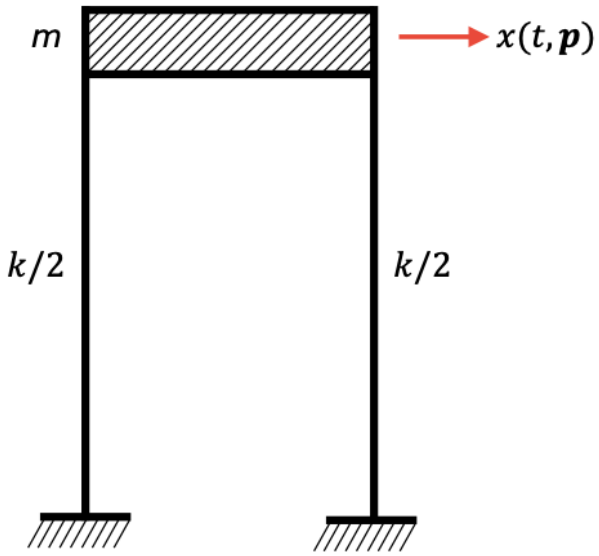

Figure 4-1: Graphical representation of the system used in example 1 [29]

4.1.1 Non-Gaussian loading

In this work, $p(t)$ is modeled by Student's t distribution, and therefore $\boldsymbol{p}$ is non-Gaussian. The Student's t distribution is characterized by three parameters [41]:

- mean μ
- scale σ_s
- degrees of freedom ν

Therefore, loading $\boldsymbol{p}$ modeled as a Student's t distribution, can be expressed as follows:

$$p(t) \sim t_\nu(\mu, \sigma_s) \tag{4-1}$$

Scale parameter σ_s relates to the standard deviation as presented below:

$$\sigma_{st.dev.} = \sigma_s \sqrt{\frac{\nu}{\nu - 2}} \tag{4-2}$$

The main parameter is a number of degrees of freedom ν. This parameter defines the shape of the Student's t distribution. In general, t-distribution has symmetric bell-shaped form, but different from the standard normal distribution curve, the t-distribution curve is flatter, has a lower height and has a wider spread [42]. The influence of each parameter on the distribution is presented in Figures 4-2, 4-3, and 4-4 [41].

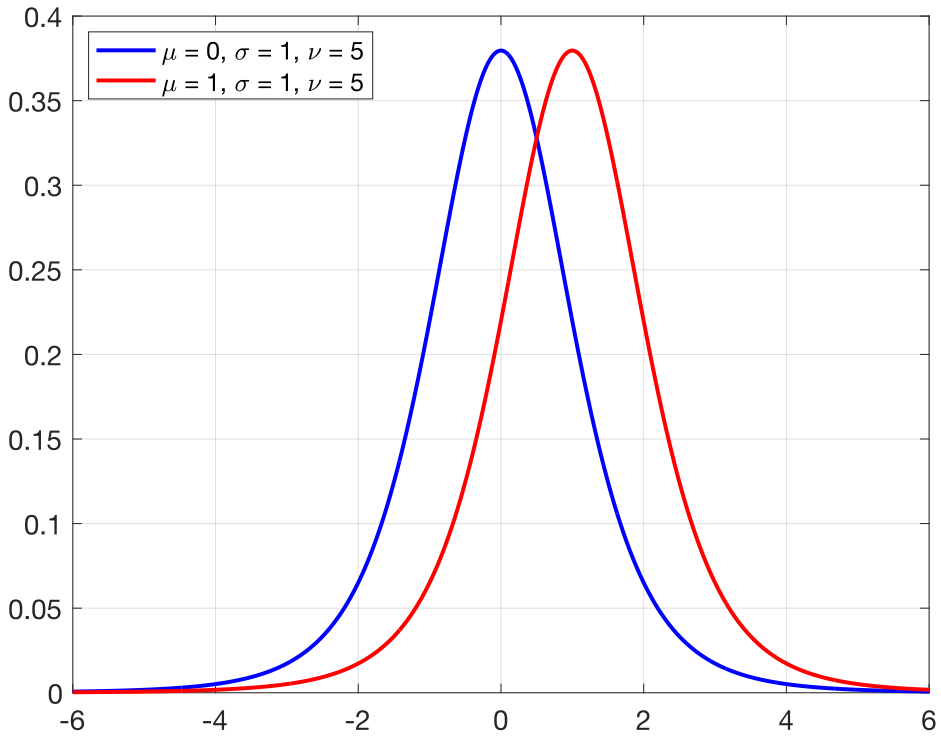

Figure 4-2: Graphical representation of the influence of mean parameter μ on the Student's t distribution

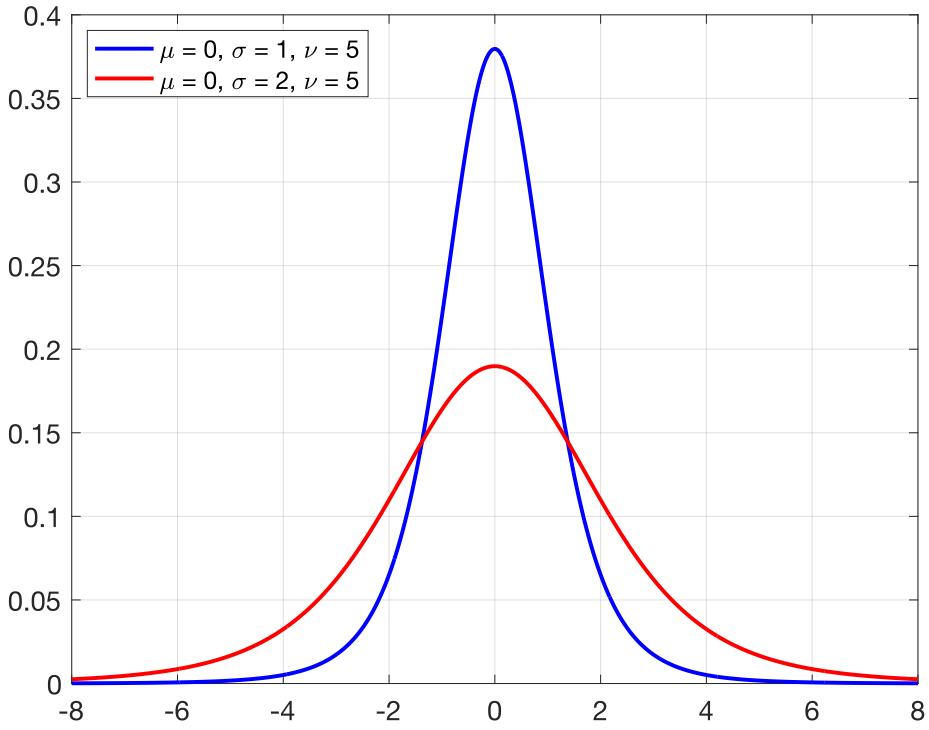

Figure 4-3: Graphical representation of the influence of scale parameter σ on the Student's t distribution

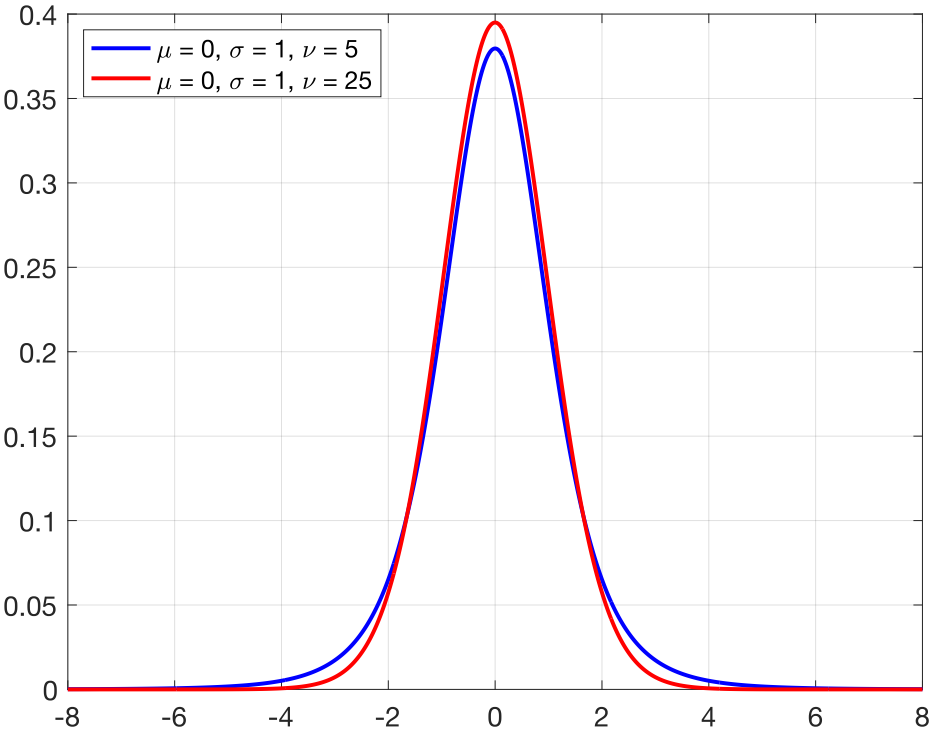

Figure 4-4: Graphical representation of the influence of the degrees of freedom parameter ν on the Student's t distribution

It is important to note that the larger the number of degrees of freedom ν, the more similar Student's t distribution is to the normal distribution, so they tend to be the same provided that $\nu \rightarrow \infty$.

4.1.2 Obtained results' discussion

First of all, input parameters for the characterization of the Student's distribution have to be discussed. The value of the scale parameter is calculated based on Eq. (4-2):

$$\sigma_s = \frac{\sigma_{st.dev.}}{\sqrt{\frac{\nu}{\nu - 2}}} \tag{4-3}$$

Then, the number of degrees of freedom ν has to be defined. As discussed previously, this parameter defines how similar Student's t distribution to a normal distribution. The following figures below are presented to show graphically how parameter ν influence a probability density function of the Student's distribution.

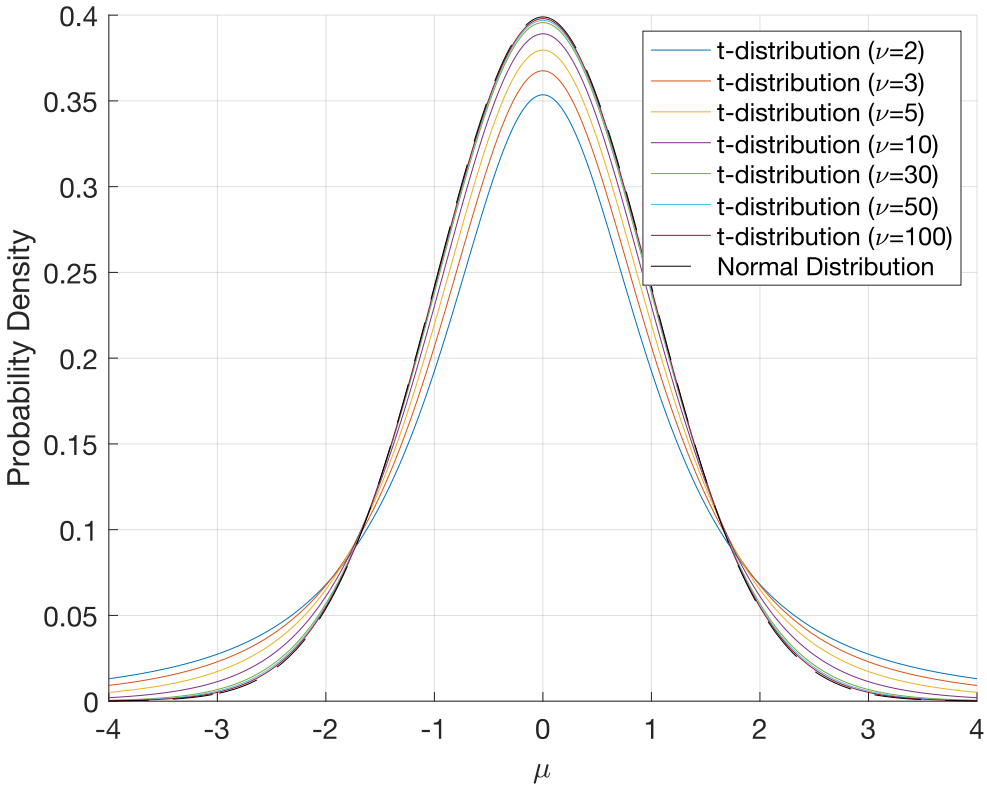

Figure 4-5: Comparison of probability density function of the normal distribution and Student's t distribution for different values of ν

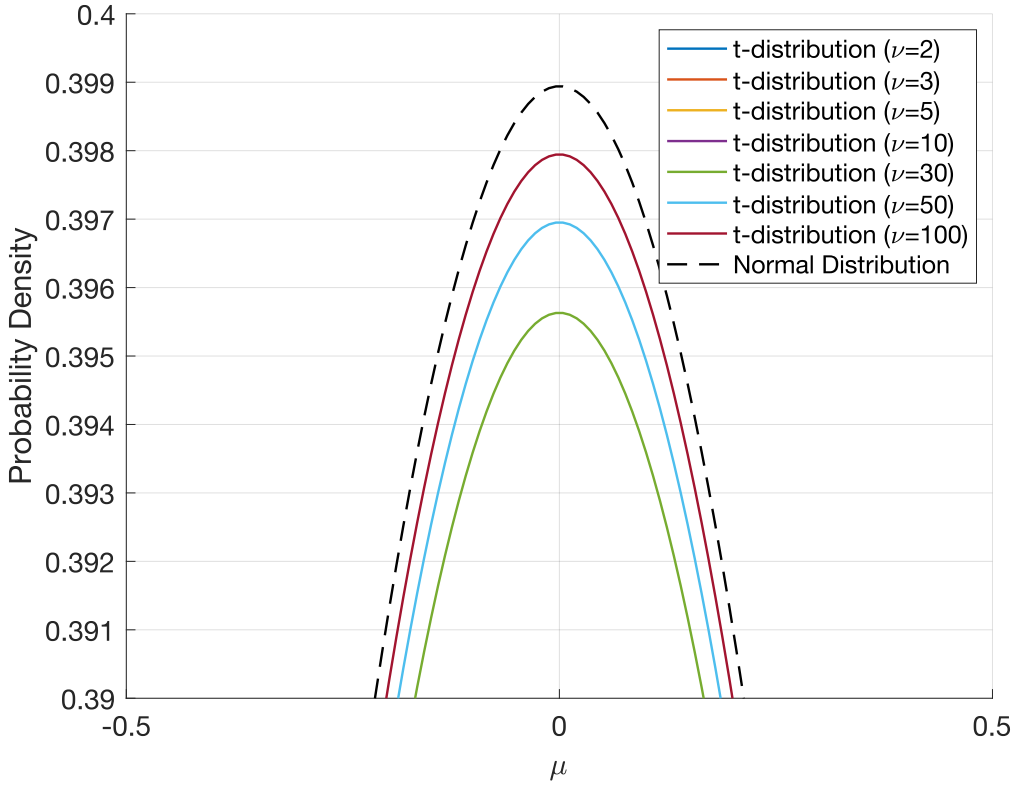

Figure 4-6: Zoomed comparison of probability density function of the normal distribution and Student's t distribution for different values of ν

The next step is to analyze Gaussianisation accuracy for different parameters ν of Student's t distribution. In order to do so, one sample of uniformly distributed random numbers $\boldsymbol{u}\sim U[0;1]$ is generated. Using this generated sample and different values of ν, both responses of the system are now calculated – exact non-Gaussian response and Gaussianised response. Exact non-Gaussian response of the system can be calculated by means of Eq. (3-9) and a Gaussianised response of the system is calculated by means of Eq. (3-88). Since one generated sample $\boldsymbol{u}$ is used for the calculation of both responses, equation for the calculation of the exact non-Gaussian loading would obtain the following appearance:

$$\boldsymbol{x}_i = \boldsymbol{A}_i \boldsymbol{p}(\boldsymbol{u}) \tag{4-4}$$

where loading $\boldsymbol{p}$ is calculated by means of the inverse-uniform transformation such as:

$$\boldsymbol{p} = \mu + \sigma_s \cdot F_p^{-1}(\boldsymbol{u}, \nu) \tag{4-5}$$

where $F_p^{-1}(\boldsymbol{u}, \nu)$ represents the inverse cumulative distribution function of the Student's t distribution associated with $\boldsymbol{u}$ and with respect to degrees of freedom ν.

Respectively, the Gaussianised response is calculated with respect to Eq. (3-88), where $\boldsymbol{z}$ is calculated as:

$$\boldsymbol{z} = F_{\boldsymbol{z}}^{-1}(\boldsymbol{u}) \tag{4-6}$$

where F_z^{-1} is a inverse cumulative distribution function associated with $\boldsymbol{z}$.

On the following Figures, non-Gaussian response of the system as well as Gaussianised response of the system are compared to each other with respect to different parameters of ν in order to evaluate the accuracy of the Gaussian approximation.

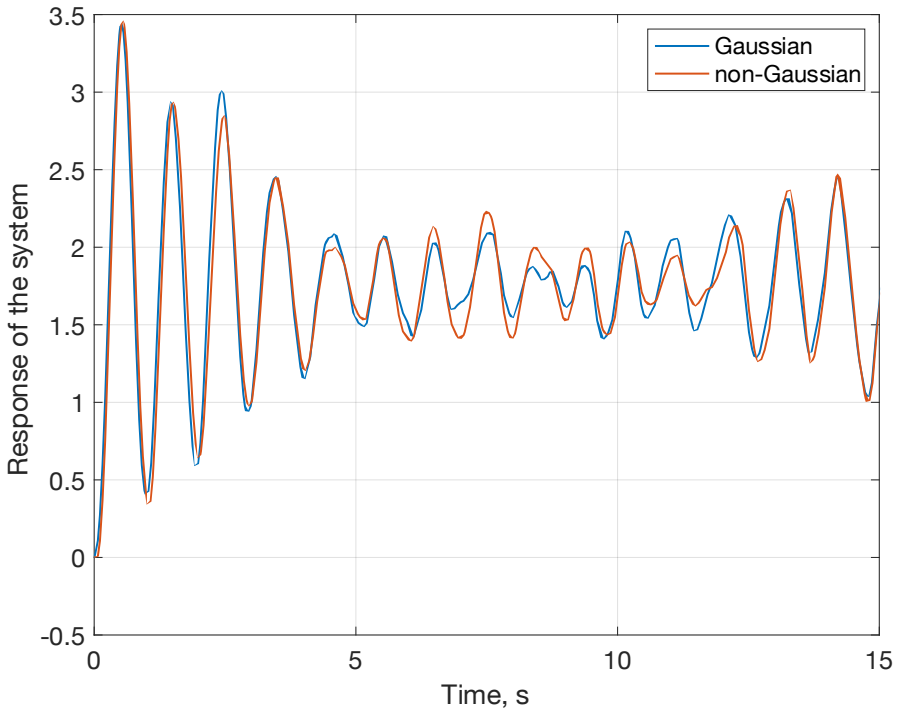

Figure 4-7: Comparison of the system response under Gaussian and non-Gaussian loadings for $\nu = 3$

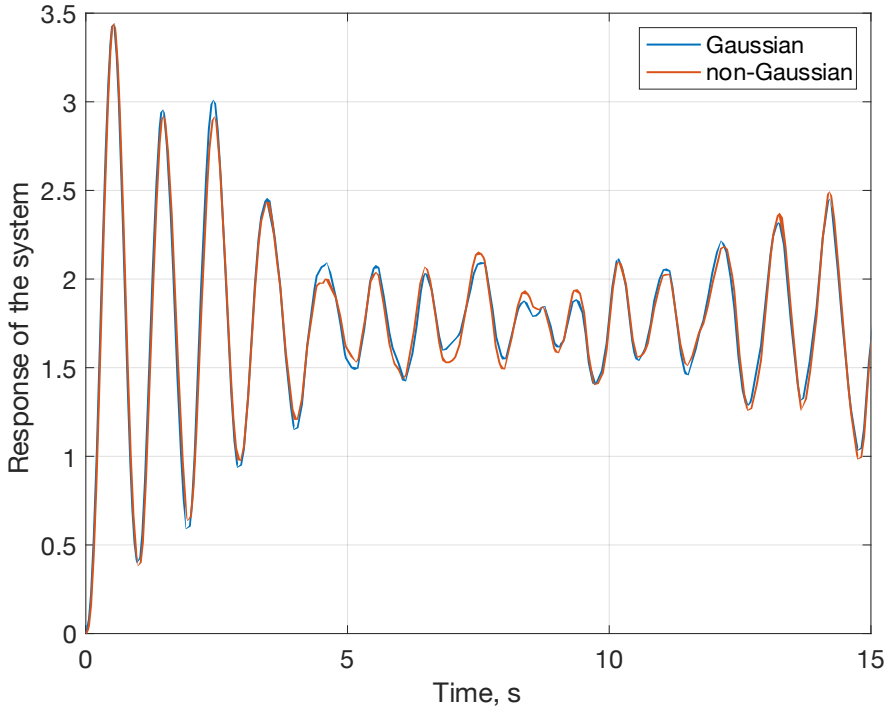

Figure 4-8: Comparison of the system response under Gaussian and non-Gaussian loadings for $\nu = 5$

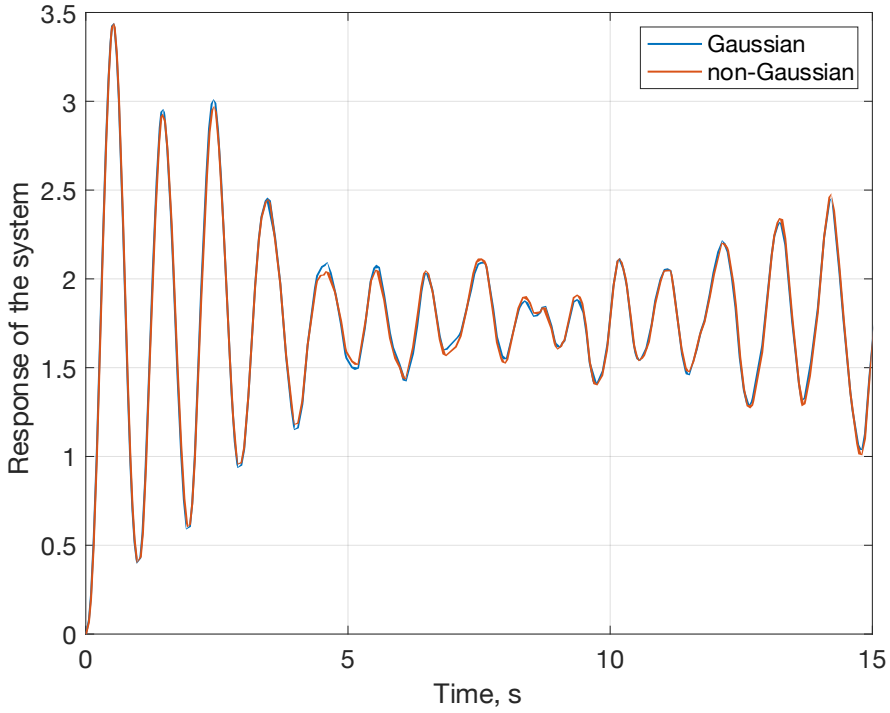

Figure 4-9: Comparison of the system response under Gaussian and non-Gaussian loadings for $\nu = 10$

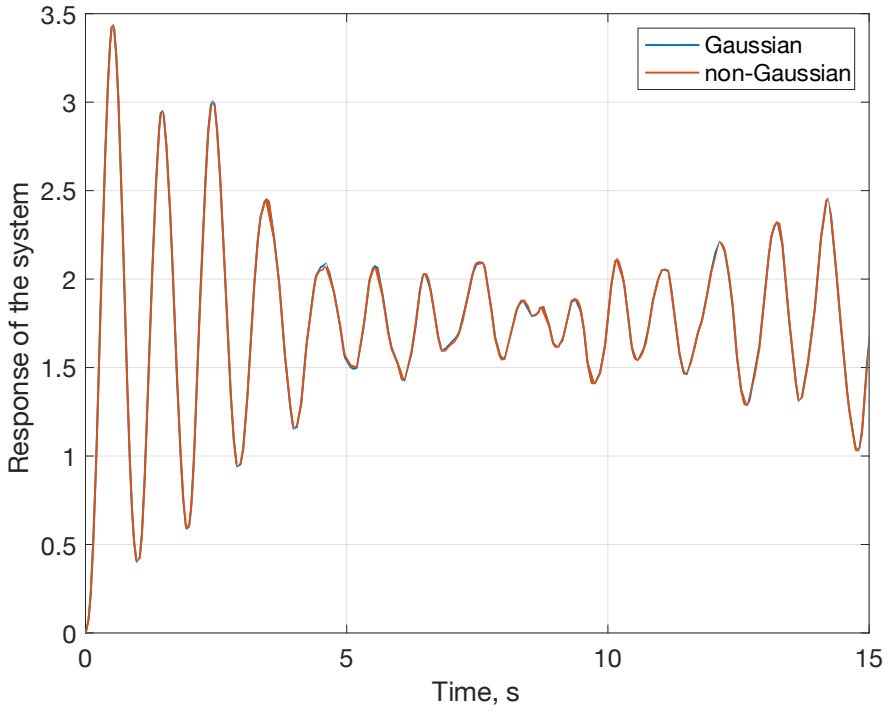

Figure 4-10: Comparison of the system response under Gaussian and non-Gaussian loadings for $\nu = 30$

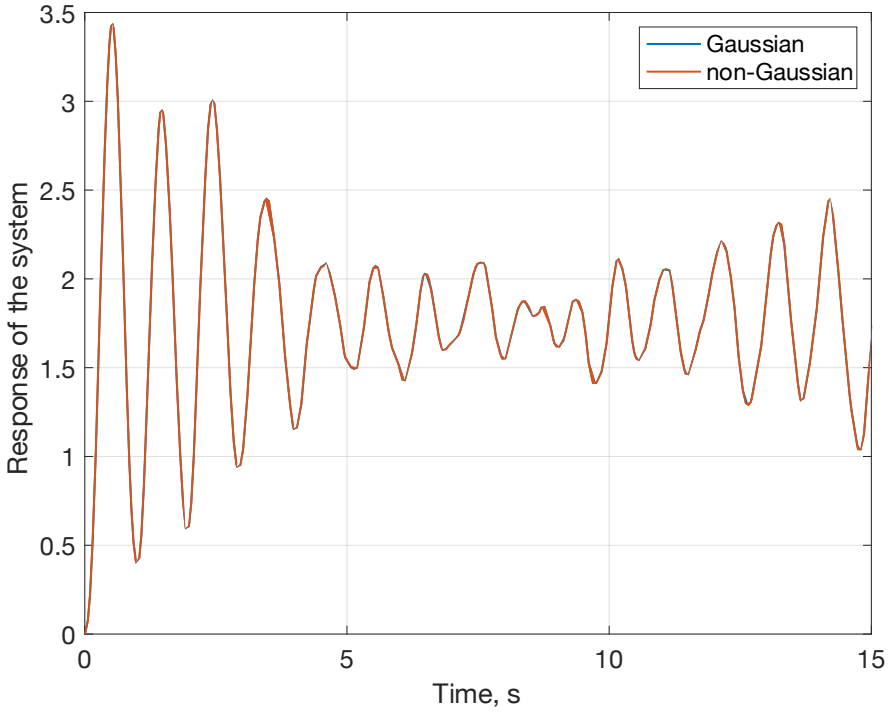

Figure 4-11: Comparison of the system response under Gaussian and non-Gaussian loadings for $\nu = 100$

As can be seen from the Figures above, the larger value of parameter ν, the more accurate Gaussian approximation becomes. This can be explained by the fact that at low ν values Student's t distribution has heavier tails compared to the Gaussian distribution. Respectively, as the degrees of freedom parameter increases, the Student's t distribution's tails become less heavy, and the distribution increasingly resembles a Gaussian distribution. As might be deduced from the figures above, starting from $\nu = 30$, Student's t distribution and a normal distribution tend to converge. Since the main idea is to approximate non-Gaussian loading accurately enough, in the presented examples the number of degrees of freedom is set to 30.

The thresholds for up-crossing and down-crossing are set to be $b_1 = 4.3m$ and $b_2 = -0.8m$, respectively.

Applying the procedure of Importance Sampling Using Reference Points as discussed in subsection 3.2.4, weights for every time instance are obtained as presented in Figure 4-12. Weights with such small values indicate that at the majority of time steps the system is far away from the specified failure thresholds, which also means that they contribute minimally to the failure.

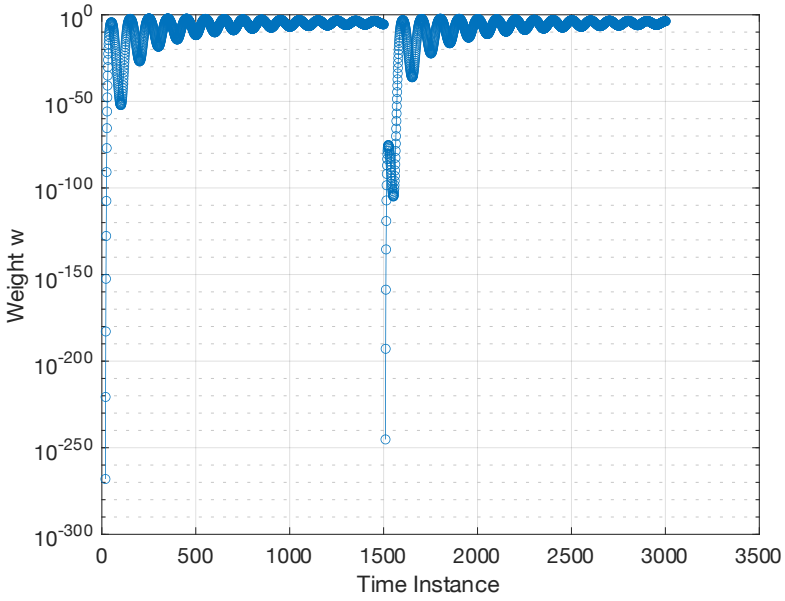

Figure 4-12: Weights in logarithmic representation

Then, the samples are generated, and the failure event of the system is investigated with respect to the specified thresholds b_1 and b_2. After that, weights for every one of the $N = 10^4$ samples are calculated with the implementation of the "log-sum-exp" trick discussed in sub-section 3.2.4 and specifically Eq. (3-97). For the specified input data and set parameters, the failure probability of the system is estimated as 5.49×10^{-3} with the coefficient of variation being equal to 1.95%. To validate the accuracy of obtained results using ISURP, Monte Carlo Simulation is also performed with 10^5 samples being generated. Failure probability obtained from Monte Carlo Simulation is 5.20×10^{-3}. Comparison and the evolution of the obtained results are shown in Figure 4-13.

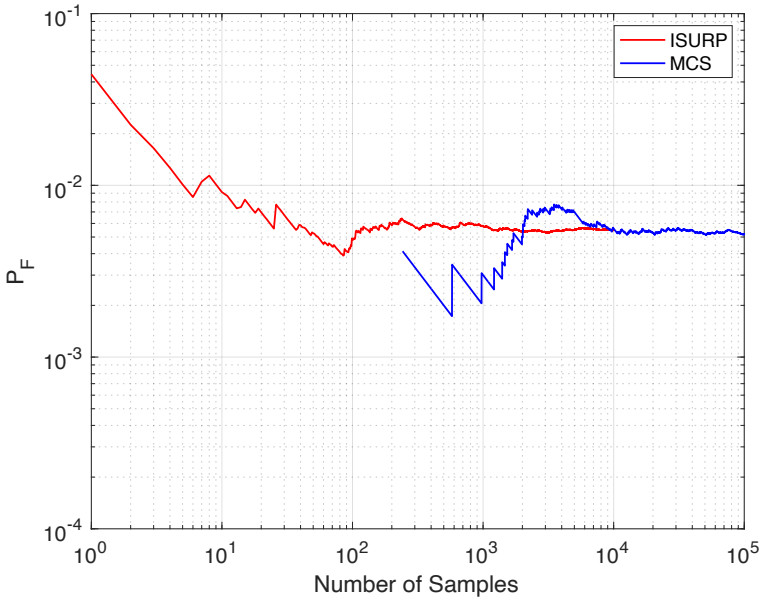

Figure 4-13: Evolution of the failure probability using ISURP and MCS for SDOF system

For illustration purposes, thresholds are modified, such as $b_1 = 0.022m$ and $b_2 = 0.006m$ to enable the sample generation in two-dimensional space. This allows to visually represent limit state functions, reference points, and generated samples at time step $t = 2\Delta t = 0.02s$. Samples are generated both in Gaussian and Physical spaces, which is shown in the figures below.

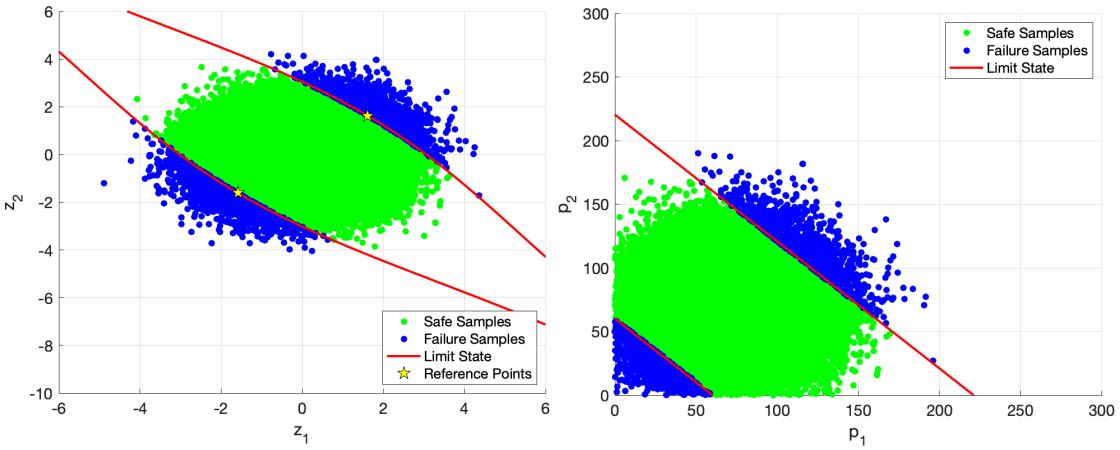

(a) Gaussian space

(b) Physical space

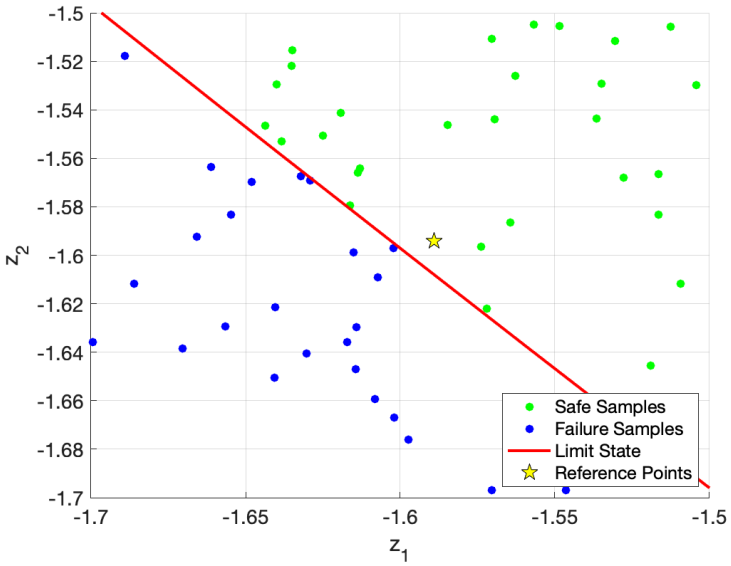

(c) Zoomed Gaussian space

Figure 4-14: Samples generated in example 1

Presented above Figure 4-14 demonstrates obtained limit state functions for the 2D case, defined reference points and generated samples. Since the non-Gaussianity of the Student's t loading is weak due to the selected parameter $\nu = 30$, reference points just slightly deviate from the limit state, as shown in Figure 4-14 (c).

4.1.3 Influence of non-Gaussianity

As discussed previously, the main parameter of the Student's t distribution is a number of degrees of freedom ν, that defines the non-Gaussianity of the distribution. In order to investigate the

influence of non-Gaussianity on the estimation of the failure probability of the system, Importance Sampling Using Reference Points is performed using 10^4 samples for different values of ν parameter mentioned in sub-section 4.1.2. To be more specific, simulations are performed for the same thresholds $b_1 = 4.3m$ and $b_2 = -0.8m$, and for different values of ν, such as 3, 5, 10, 30, and 100. For the validation of the obtained results, Monte Carlo Simulation is also performed for the specified values of ν using 10^5 samples. Obtained results and their comparison are shown in Table 4-1. Specifically, Probability of Failure (PF) and a Coefficient of Variation (COV) obtained by ISURP method as well as PF obtained by MCS are presented in the table.

Table 4-1: Results of SDOF example obtained by ISURP and MCS

Result	$\nu = 3$	$\nu = 5$	$\nu = 10$	$\nu = 30$	$\nu = 100$
PF - ISURP	1.23×10^{-2}	6.13×10^{-3}	5.57×10^{-3}	5.49×10^{-3}	5.47×10^{-3}
PF - MCS	1.28×10^{-2}	5.83×10^{-3}	5.32×10^{-3}	5.20×10^{-3}	5.24×10^{-3}
COV	7.95%	3.25%	2.03%	1.95%	1.95%

Only for $\nu = 3$, the simulation using ISURP is performed with 10^5 samples since 10^4 was not enough to see the stabilization of the failure probability. This is due to strongly non-Gaussian behavior explained by small number of degrees of freedom ($\nu = 3$) of the Student's t distribution. In general, as can be seen from the obtained results, the lower the value of ν parameter - the higher the value of failure probability and the worse ISURP performs, meaning that there is more variability in the estimates, which is the consequence of the Gaussianisation. Graphical comparison of the obtained evolution of failure probabilities is presented in Fig. 4-15 (a-e). Additionally, Fig. 4-16 (a-e) presents evolution of COV using ISURP for every specified value of ν parameter. Figure 4-16 (a) confirms that the ISURP performs not so good for small values of ν parameter and specifically $\nu = 3$. Given the sudden jumps in COV, it means that the importance sampling density is not the optimal one. In comparison with the other COV figures, for higher ν parameters the evolution of coefficient of variation is quite smooth, showing that for higher ν parameters ISURP performs better due to reasonable Gaussianisation.

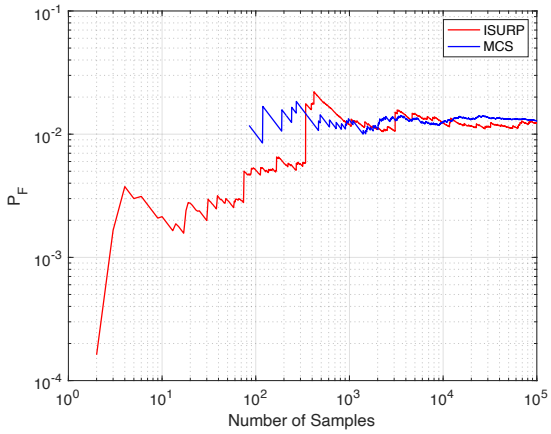

(a) $\nu = 3$

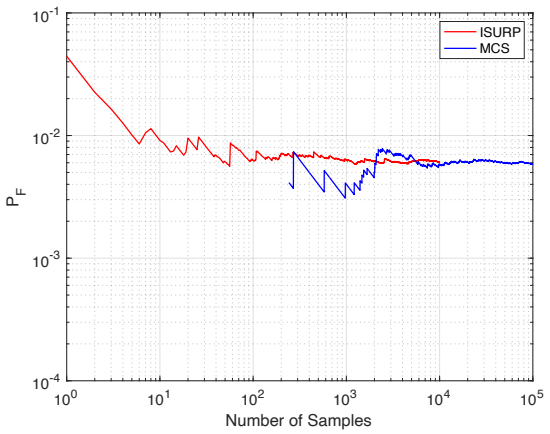

(b) $\nu = 5$

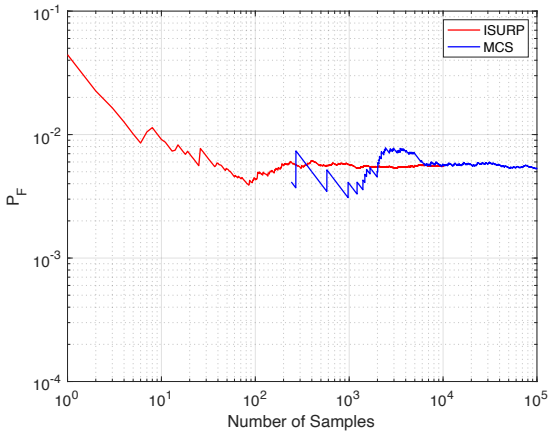

(c) $\nu = 10$

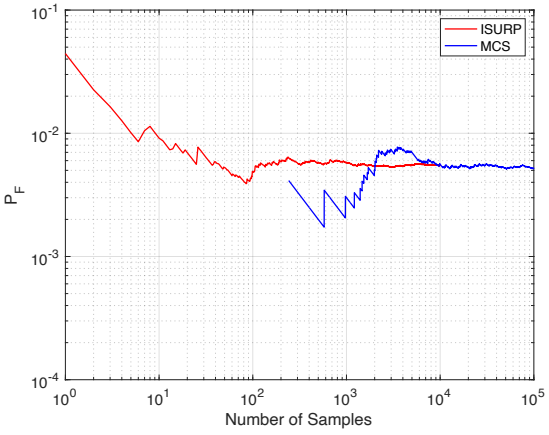

(d) $\nu = 30$

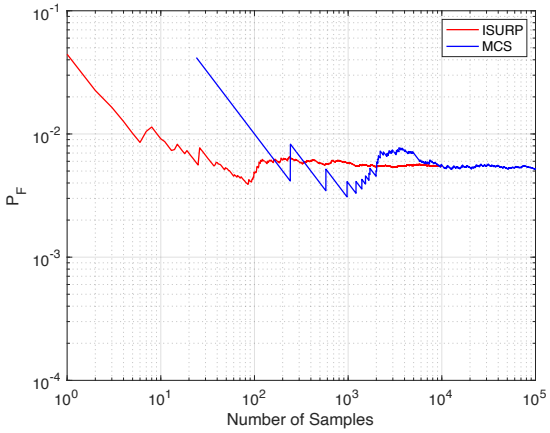

(e) $\nu = 100$

Figure 4-15: Evolution of the failure probability for different values of ν parameter for SDOF system

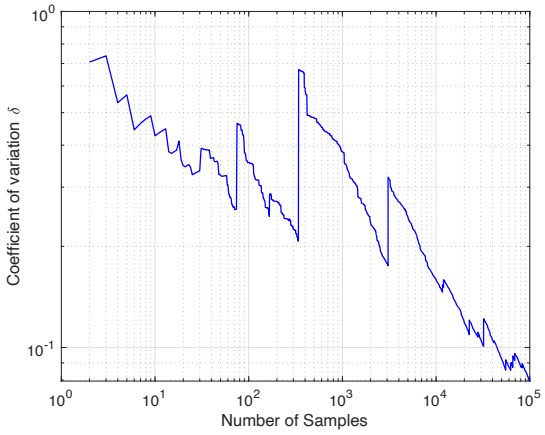

(a) $\nu = 3$

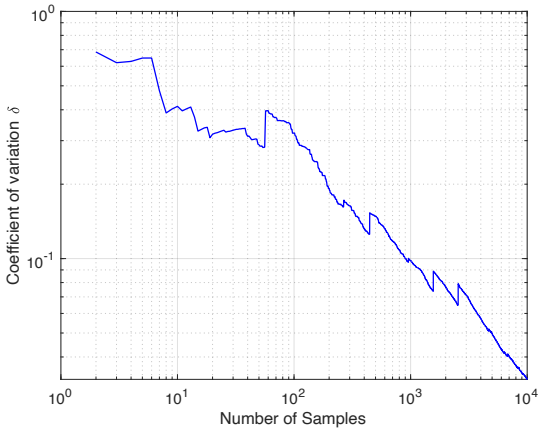

(b) $\nu = 5$

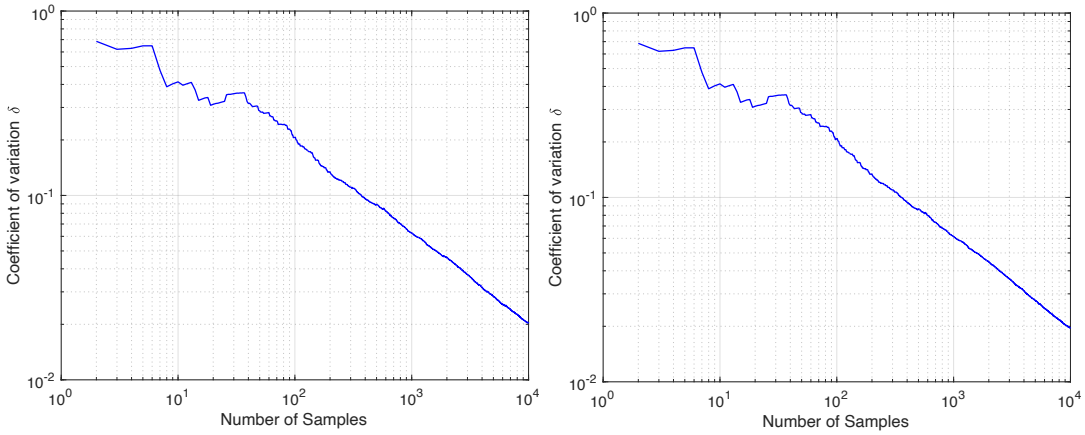

(c) $\nu = 10$ (d) $\nu = 30$

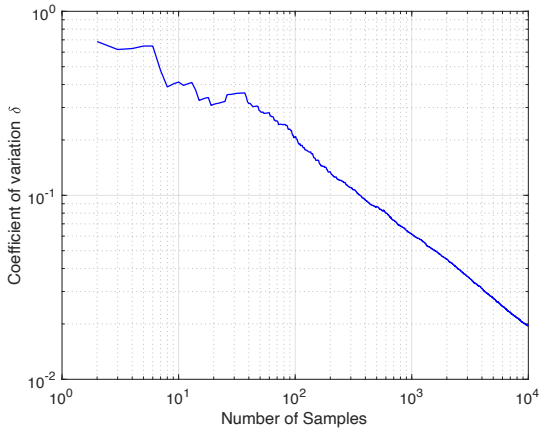

(e) $\nu = 100$

Figure 4-16: Evolution of the coefficient of variation for different values of ν parameter for SDOF system

4.2 Two degree of freedom (TDOF) system

The second example is focused on the two degree of freedom system and specifically the two-story shear beam structure shown in Fig. 4-17 [29]. The masses, stiffness, and the classical damping ratios of two floors are assumed to be equal and have the values $m_1 = m_2 = 30 \times 10^3 kg$, $k_1 = k_2 = 18 \times 10^6 N/m$ and $d_1 = d_2 = 4\%$. Relative displacement of the first and second floors with respect to the ground, as well as the interstory displacement, are taken as responses of interest. The system is subjected to a non-Gaussian white noise following a Student's t distributed force with the spectral intensity $S = 10^{-4}\ m^2/s^3$, duration $T = 15s$, and a discrete time step $\Delta t = 0.01s$ that corresponds to the spectral density $2\pi S/\Delta t$. Applied force is characterized by a mean value $\mu = 0.7$ and a standard deviation $\sigma_{std.dev.} = \sqrt{2\pi S/\Delta t}$. Estimation of the first excursion probability of the system is considered to be the main objective.

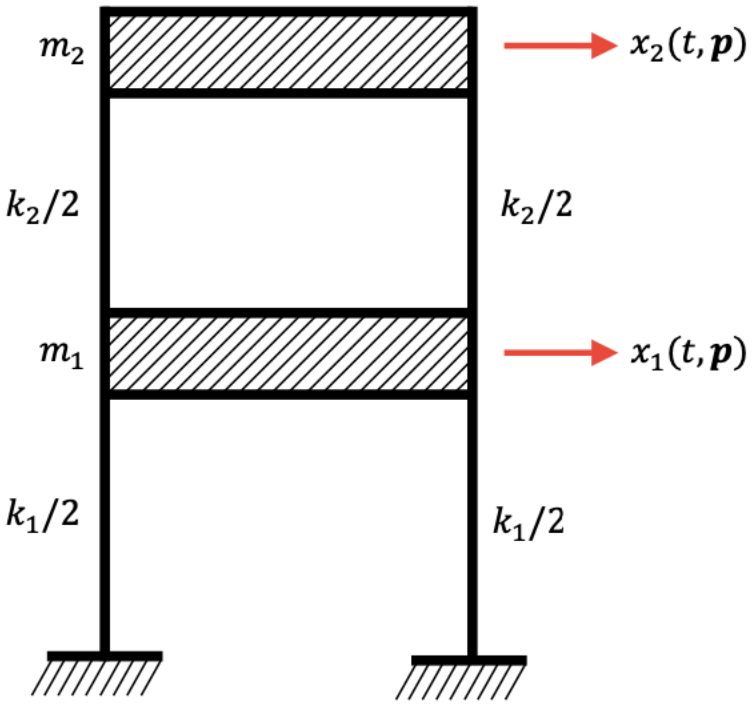

Figure 4-17: Graphical representation of the system used in example 2 [29]

4.2.1 Obtained results' discussion

The same as for example 1, the Student's t distribution characterizing parameters and specifically degrees of freedom parameter ν have to be specified. In order to investigate the influence of ν on the accuracy of the Gaussianisation, a comparison between the Gaussian and non-Gaussian responses of the system is shown below. In this case, the first response of interest is considered. Following the procedure described in example 1, a sample of uniformly distributed random numbers $\boldsymbol{u}\sim U[0;1]$ is generated. Based on this generated sample, a non-Gaussian response as well Gaussianised response of the system are calculated.

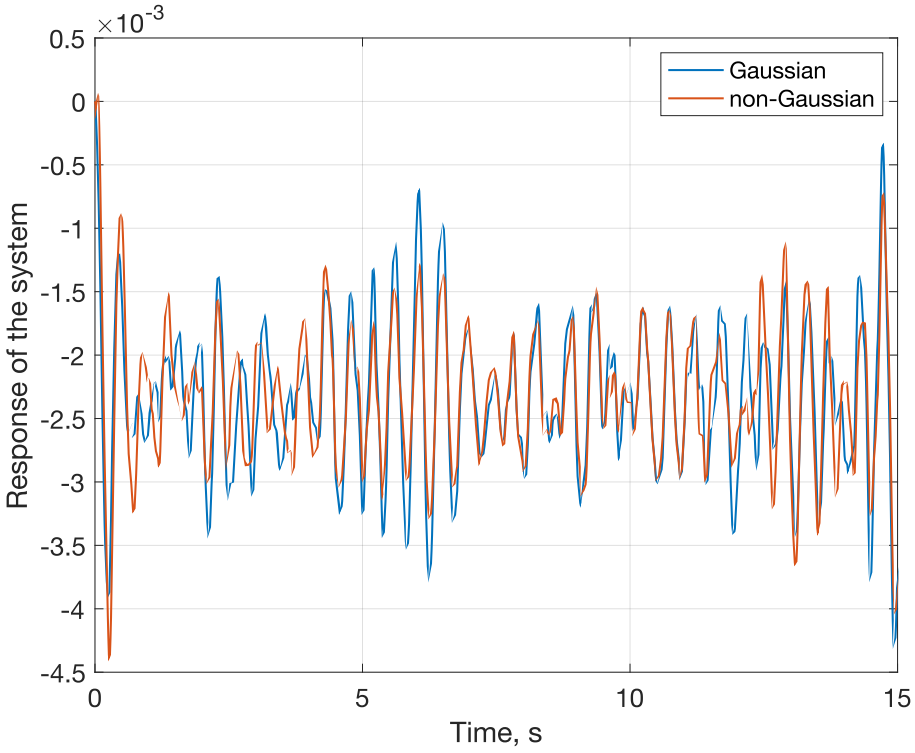

Figure 4-18: Comparison of the first response of interest under Gaussian and non-Gaussian loadings for $\nu = 3$

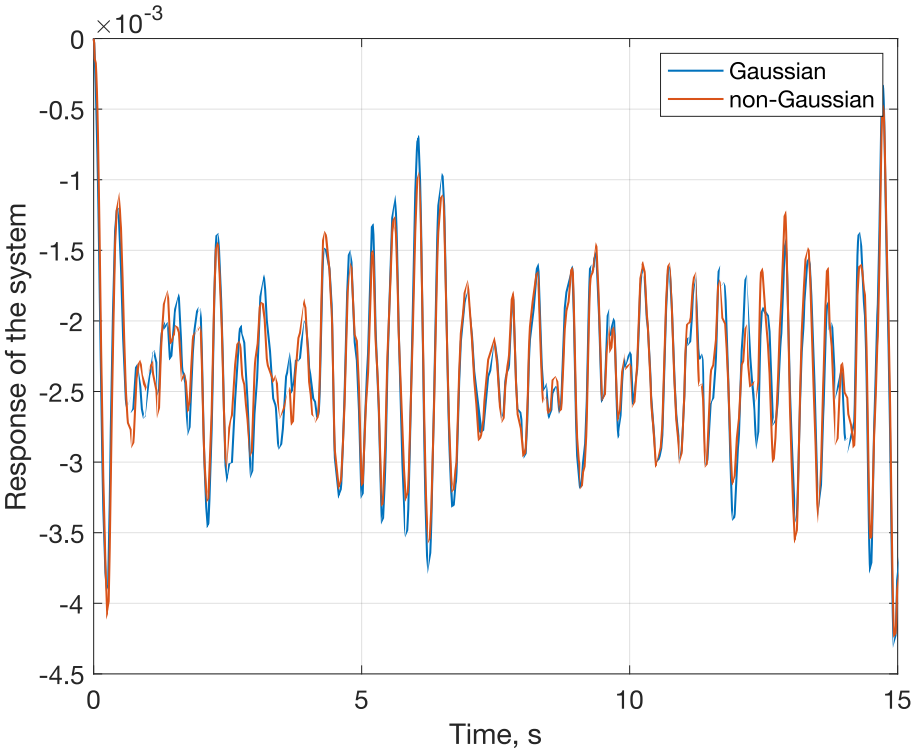

Figure 4-19: Comparison of the first response of interest under Gaussian and non-Gaussian loadings for $\nu = 5$

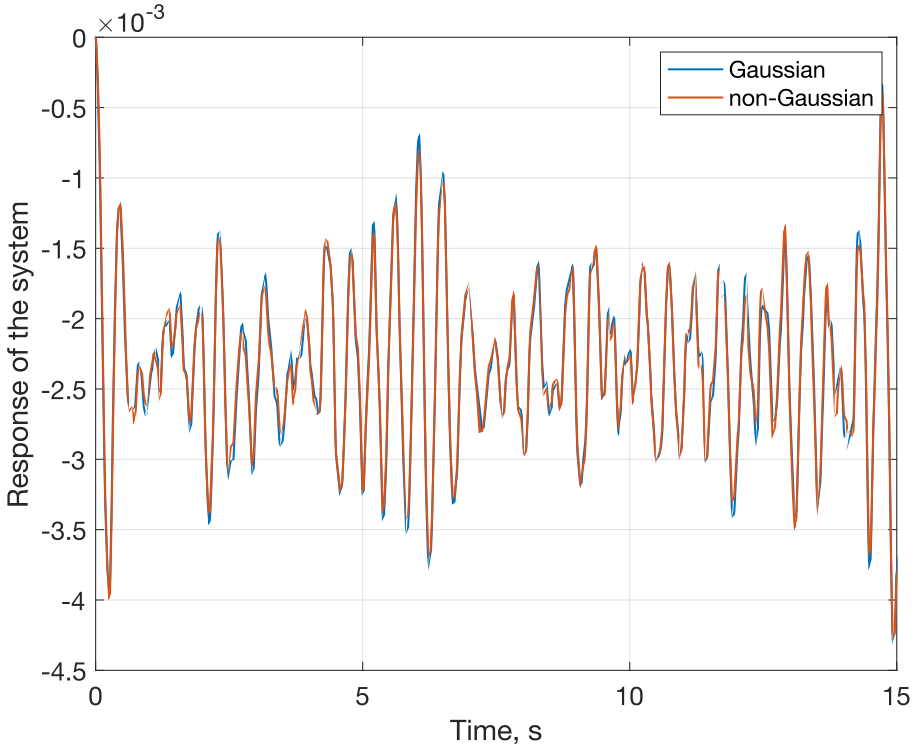

Figure 4-20: Comparison of the first response of interest under Gaussian and non-Gaussian loadings for $\nu = 10$

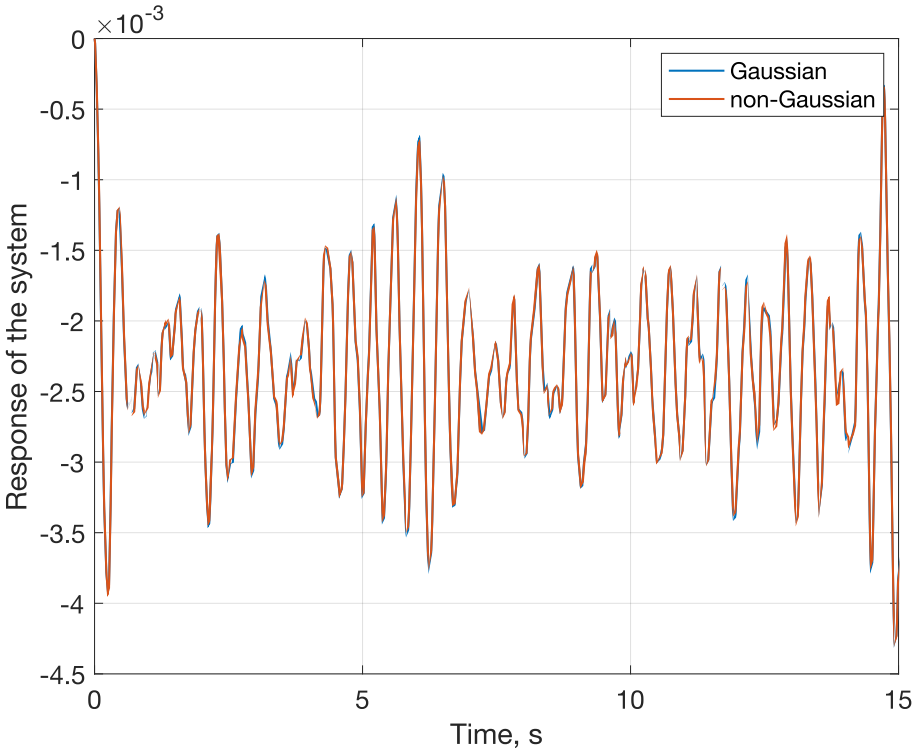

Figure 4-21: Comparison of the first response of interest under Gaussian and non-Gaussian loadings for $\nu = 30$

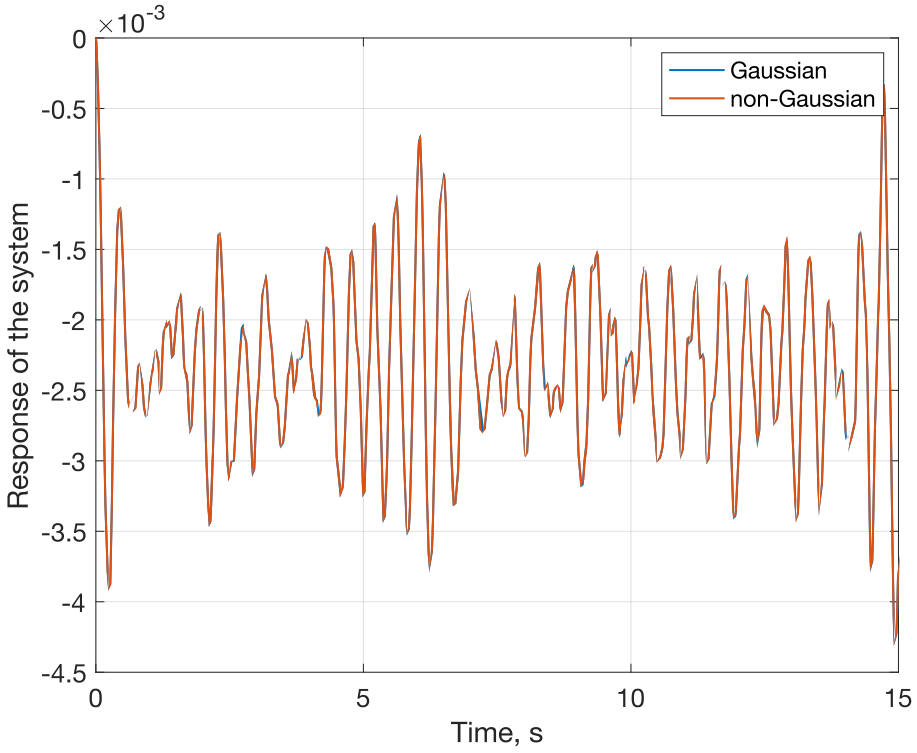

Figure 4-22: Comparison of the first response of interest under Gaussian and non-Gaussian loadings for $\nu = 100$

As can be seen from the Figures above, the larger value of parameter ν, the more accurate Gaussian approximation becomes. Therefore, ν is set to 30 as the optimum value to obtain accurate enough Gaussian approximation of the original non-Gaussian loading, and therefore, this value is used in simulations for this example.

The thresholds for up-crossing and down-crossing are set to be $b_1 = 0.0022m$ and $b_2 = -0.009m$, respectively.

Applying the procedure of Importance Sampling Using Reference Points as discussed in subsection 3.2.4, weights for every time instance are obtained as presented in Figure 4-23. As can be seen, values of the calculated weights are quite small. It means that for the most number of time steps the displacement of the system is far away from the specified failure thresholds, and therefore, their contribution to the failure is quite small.

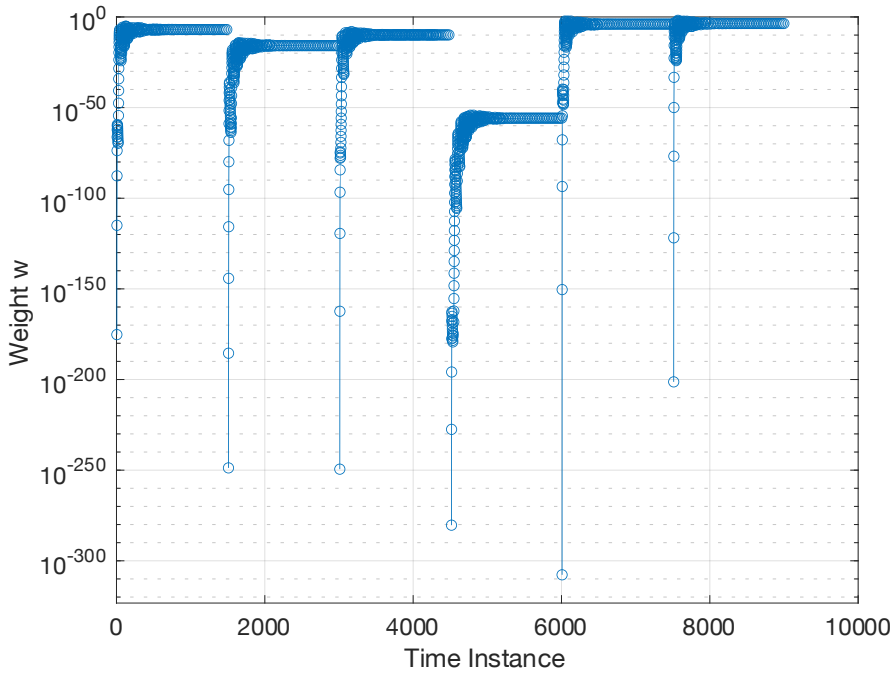

Figure 4-23: Weights in logarithmic representation

Based on all the obtained results, the failure probability of the system is estimated by means of Importance Sampling Using Reference Points with 10^4 samples and is equal to 3.95×10^{-3} with coefficient of variation being equal to 2.07%. In order to validate the results, the failure probability of the system is also estimated by means of Monte Carlo Simulation using 10^6 samples, which gives a result of 4.32×10^{-3}. The evolution of the failure probability is presented in the figure below.

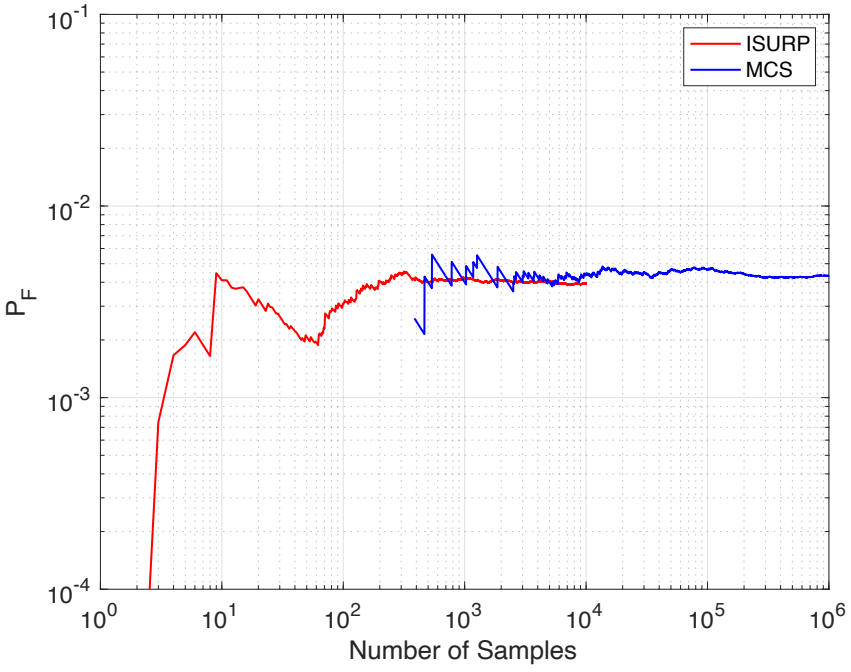

Figure 4-24: Evolution of the failure probability using ISURP and MCS for TDOF system

4.2.2 Influence of non-Gaussianity

This sub-section investigates the influence of non-Gaussianity on the estimation of the failure probability of the two degree of freedom system. To be more specific, simulation using ISURP with number of samples 10^4 is performed for the same thresholds $b_1 = 0.0022m$ and $b_2 = -0.009m$, and for different values of ν, such as 3, 5, 10, 30, and 100. For the validation of the obtained results, a Monte Carlo Simulation using 10^6 samples is performed for the same thresholds and for all the specified ν parameters. Obtained results and their comparison are presented in Table 4-2.

Table 4-2: Results of TDOF example obtained by ISURP and MCS

Result	$\nu = 3$	$\nu = 5$	$\nu = 10$	$\nu = 30$	$\nu = 100$
PF - ISURP	4.50×10^{-2}	7.53×10^{-3}	4.30×10^{-3}	3.95×10^{-3}	3.90×10^{-3}
PF - MCS	4.87×10^{-2}	7.84×10^{-3}	4.72×10^{-3}	4.32×10^{-3}	4.27×10^{-3}
COV	8.18%	4.77%	2.47%	2.07%	2.06%

As was explained in example 1, for $\nu = 3$ and $\nu = 5$, the simulation using ISURP is performed with 10^5 samples. Obtained results show that the lower the value of ν parameter - the higher the value of failure probability and the worse ISURP performs, which is also seen and explained in example 1. Graphical comparison of the obtained evolution of failure probabilities is presented in Fig. 4-25 (a-e). Additionally, Fig. 4-26 (a-e) presents evolution of COV using ISURP for every specified value of ν parameter. As can be seen in Figure 4-26 (a) and 4-26 (b), ISURP performs not so good for small values of ν parameter due to poor Gaussianisation, which is explained in example 1.

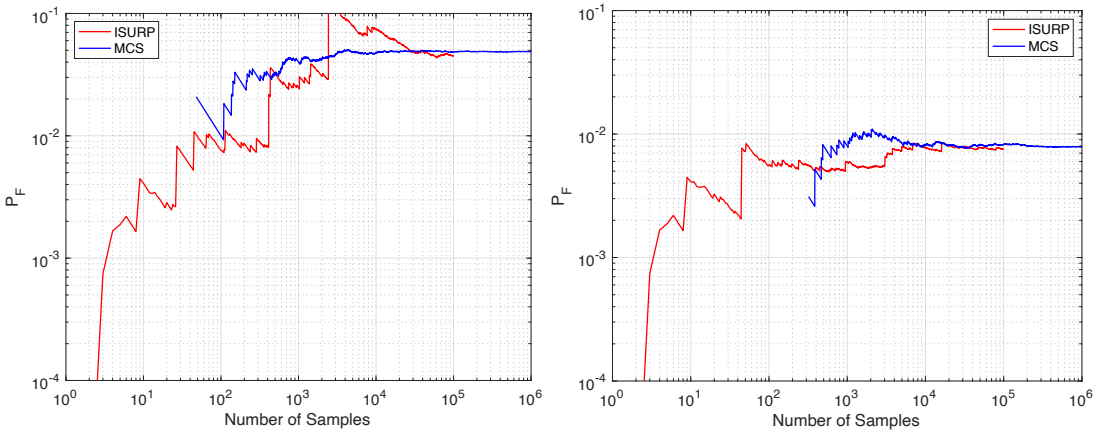

(a) $\nu = 3$ (b) $\nu = 5$

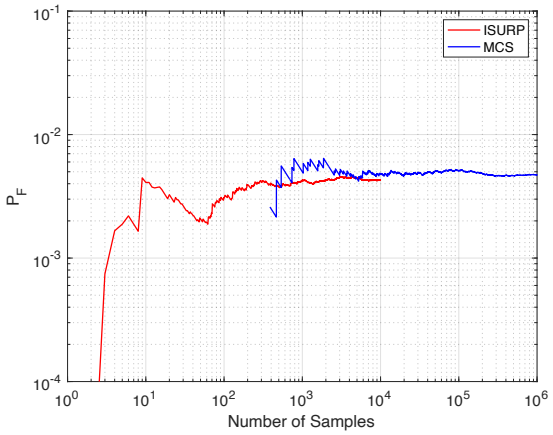

(c) $\nu = 10$

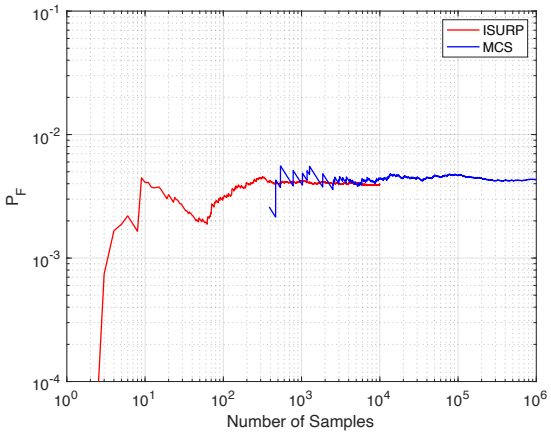

(d) $\nu = 30$

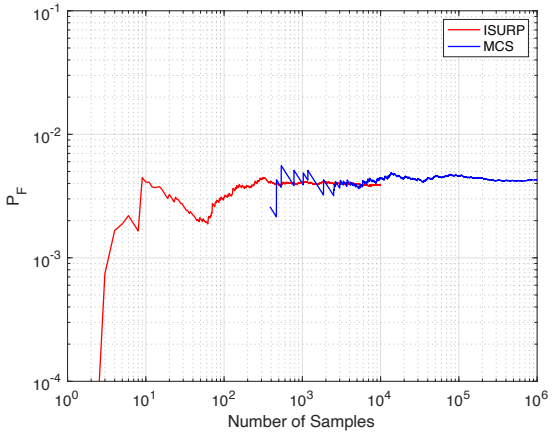

(e) $\nu = 100$

Figure 4-25: Evolution of the failure probability for different values of ν parameter for TDOF system

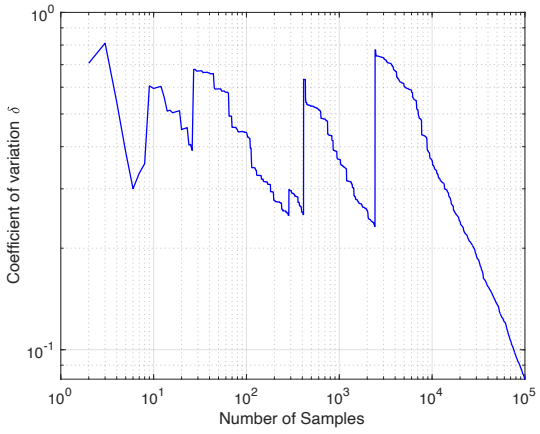

(a) $\nu = 3$

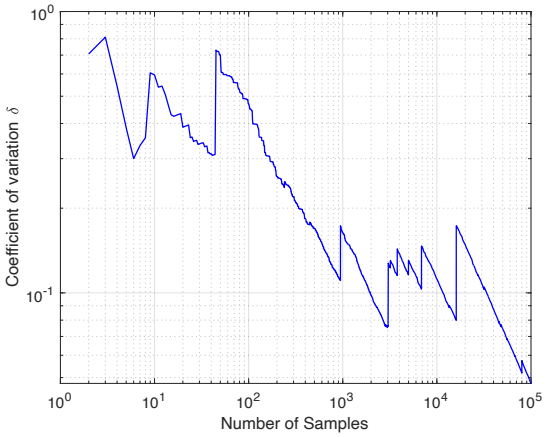

(b) $\nu = 5$

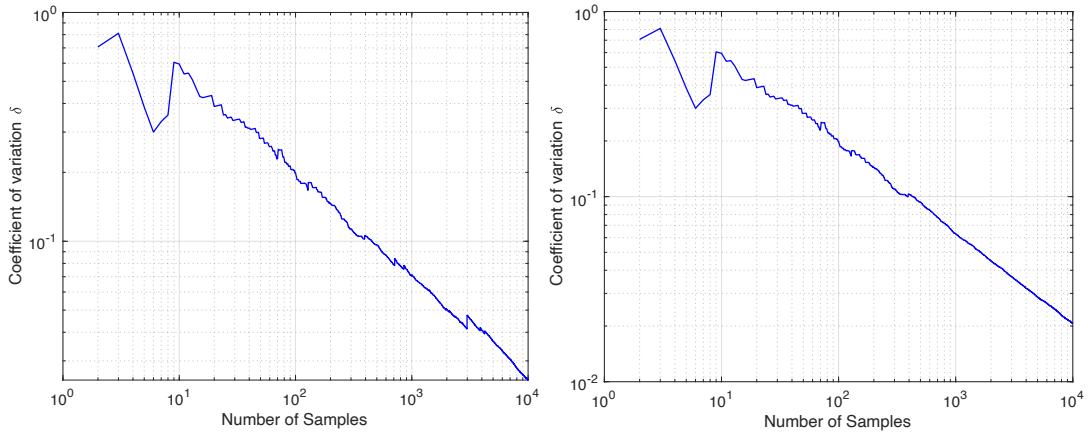

(c) $\nu = 10$ (d) $\nu = 30$

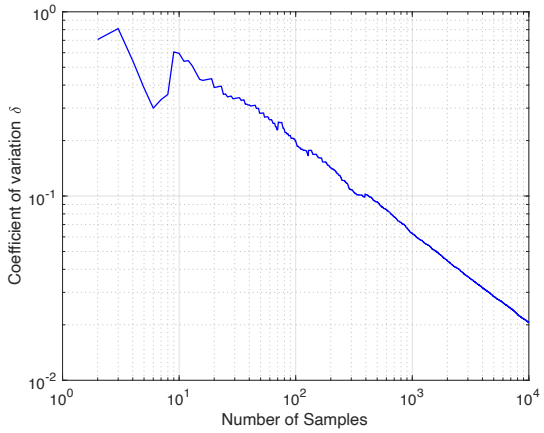

(e) $\nu = 100$

Figure 4-26: Evolution of the coefficient of variation for different values of ν parameter for TDOF system

4.3 Multi degree of freedom (MDOF) system

This example focuses on the multi degree of freedom system, which is presented in [43] and designed as a model of a milling machine tool. Therefore, in comparison to the first two examples, this example is more related to the field of manufacturing and practical applications. The presented model in Figure 4-27 is characterized by three degrees of freedom. The masses of each floor are considered to be as follows: $m_1 = 11.857kg, m_2 = 6.280kg, m_3 = 3.413kg$, where m_1 represents the mass of a bottom support together with the supporting table mass, m_2 is taken as a mass of the vertical support, and m_3 is a mass of the spindle together with the upper arm parts mass. Stiffness values are taken as follows: $k_1 = 8.81 \times 10^7\ N/m, k_2 = 5.22 \times 10^9\ N/m, k_3 = 5.17 \times 10^8\ N/m$. The system is characterized by the Rayleigh damping theory with the respective Rayleigh damping coefficients: $\alpha_R = 121.7$ and $\beta_R = 1 \times 10^{-4}$. Relative displacement of the first and the third floors with respect to the ground, as well as the interstory displacements, are taken as responses of interest. The system is subjected to a non-Gaussian white noise following a Student's t distributed force, which represents cutting force fluctuation during the

machining of ceramic matrix composites. Cutting force stochastic distribution comes from the stochasticity of fiber distribution in the material [44]. Applied to the system, force is modeled with duration $T = 0.15s$ and a discrete time step $\Delta t = 0.0001s$, since this time window is enough to capture the fluctuations of the cutting force in real cutting conditions [45, 46]. Applied in this example force is characterized by the mean value $\mu = 320$ and a standard deviation $\sigma_{std.dev.} = 0.003\mu$ [47] and a spectral intensity $S = \sigma_{std.dev.}^2 \cdot dt/(2\pi)$.

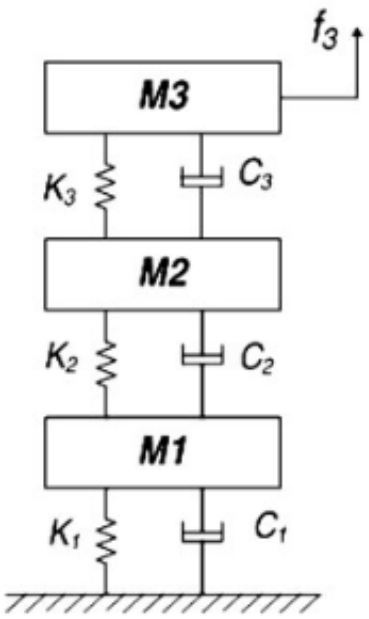

Figure 4-27: Graphical representation of the system used in example 3 [43]

4.3.1 Obtained results' discussion

As already discussed and shown in example 1 and example 2, number of degrees of freedom for the characterization of Student's distribution is set 30, which enables quite accurate Gaussianisation of the original loading. The thresholds for up-crossing and down-crossing are set to be $b_1 = 6.792 \times 10^{-6}m$ and $b_2 = -1 \times 10^{-10}m$, respectively.

Applying the procedure of Importance Sampling Using Reference Points as discussed in subsection 3.2.4, weights for every time instance are obtained as presented in Fig. 4-28. As can be seen, at the beginning of the 4th response of interest, there is a rapid increase of the weights. This can be explained by the drop of the reliability indices at the same time instants, where systems exhibits large displacement amplitude, which is close to the specified thresholds.

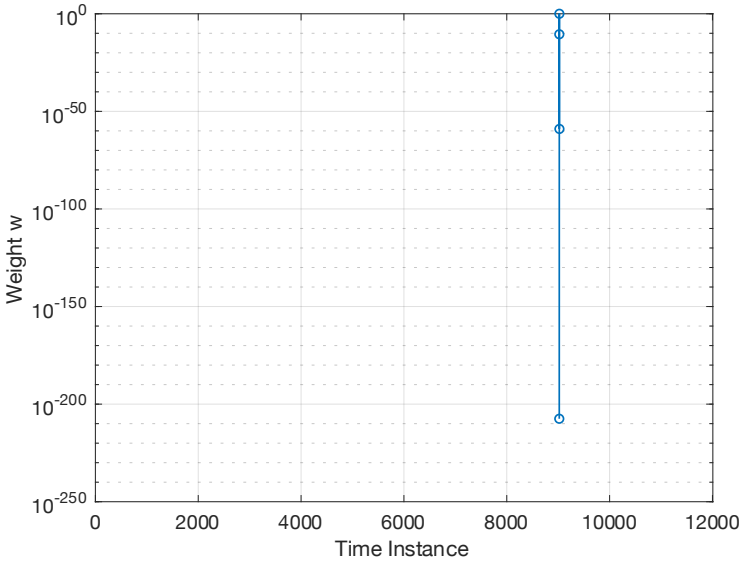

Figure 4-28: Weights in logarithmic representation

Following, the failure probability of the system is estimated by means of ISURP using 10^4 samples and is equal to 1.42×10^{-3} with the coefficient if variation being equal to 1.87% .Obtained results are validated using Monte Carlo Simulation using 10^6 samples, which gives a result of 1.48×10^{-3}. The evolution of the failure probability is presented in the figures below.

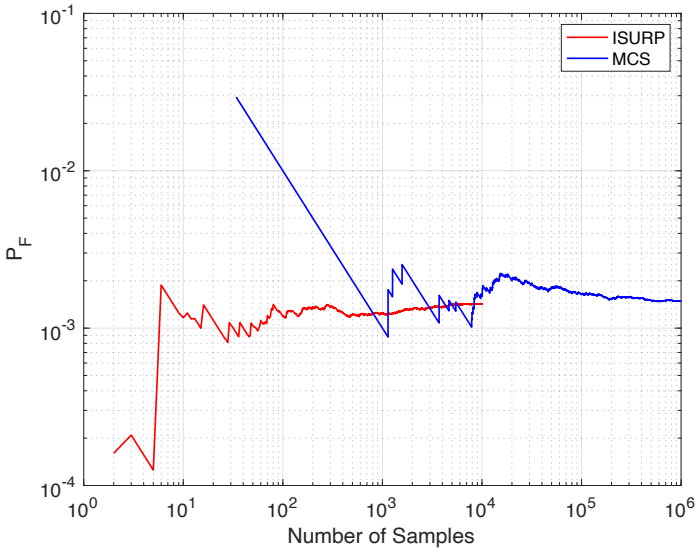

Figure 4-29: Evolution of the failure probability using ISURP and MCS for MDOF system

4.3.2 Influence of non-Gaussianity

The influence of the ν parameter on the evolution of failure probability of the MDOF system is investigated in this sub-section. Importance Sampling Using Reference Points with 10^4 samples is performed for the same thresholds $b_1 = 6.792 \times 10^{-6} m$ and $b_2 = -1 \times 10^{-10} m$, and for different values of ν, such as 3, 5, 10, 30, and 100. For the validation of the obtained results, a Monte Carlo Simulation using 10^6 samples is performed for the same thresholds and for all the specified ν parameters. Obtained results and their comparison are presented in Table 4-3.

Table 4-3: Results of MDOF example obtained by ISURP and MCS

Result	$\nu = 3$	$\nu = 5$	$\nu = 10$	$\nu = 30$	$\nu = 100$
PF - ISURP	3.89×10^{-3}	2.44×10^{-3}	1.63×10^{-3}	1.42×10^{-3}	1.39×10^{-3}
PF - MCS	4.38×10^{-3}	2.52×10^{-3}	1.69×10^{-3}	1.48×10^{-3}	1.43×10^{-3}
COV	4.18%	2.69%	2.44%	1.87%	1.85%

As already discussed in example 1 and example 2, for $\nu = 3$ and $\nu = 5$, the simulation using ISURP is performed with 10^5 samples. As can be seen from the obtained results, the lower the value of ν parameter - the higher the value of failure probability and the worse ISURP performs, which is also seen and explained in example 1. Graphical comparison of the obtained evolution of failure probabilities is presented in Fig. 4-30 (a-e). Additionally, Fig. 4-31 (a-e) presents evolution of COV using ISURP for every specified value of ν parameter. As can be seen in Figure 4-31 (a) and 4-31 (b), there are sudden jumps in coefficient of variation. Reasons of such an evolution of COV is presented in example 1.

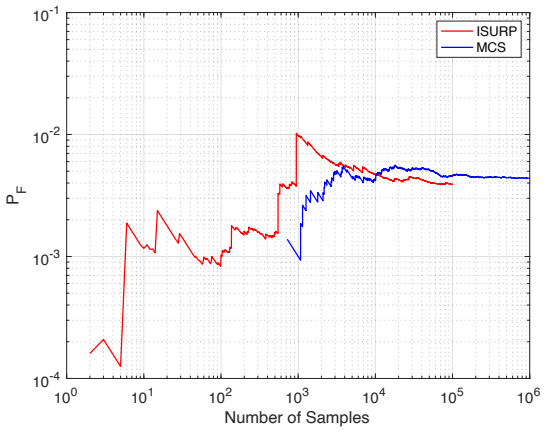

(a) $\nu = 3$

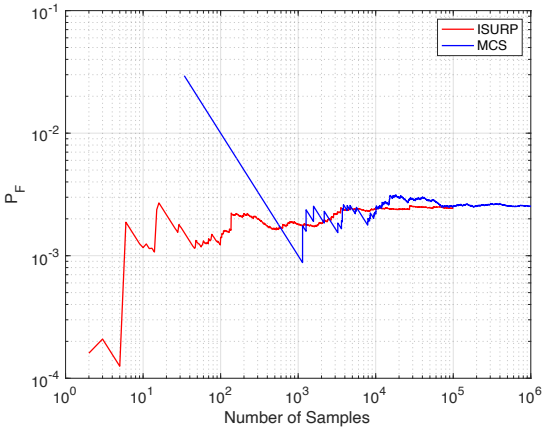

(b) $\nu = 5$

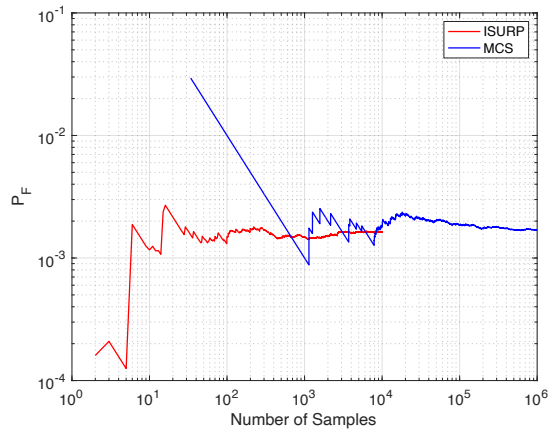

(c) $\nu = 10$

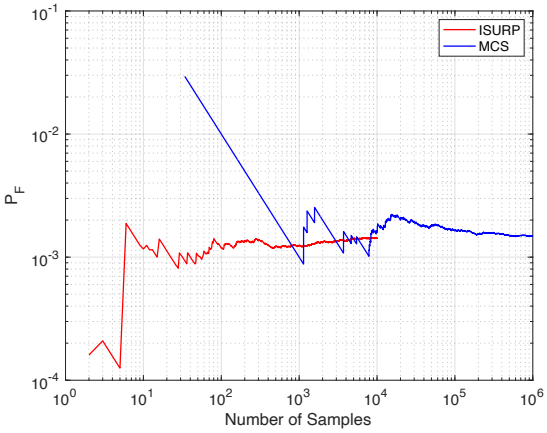

(d) $\nu = 30$

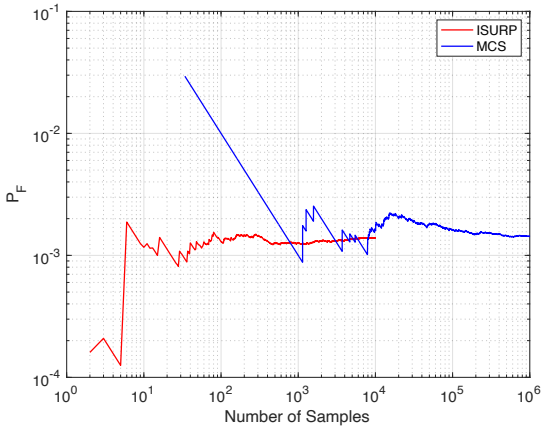

(e) $\nu = 100$

Figure 4-30: Evolution of the failure probability for different values of ν parameter for MDOF system

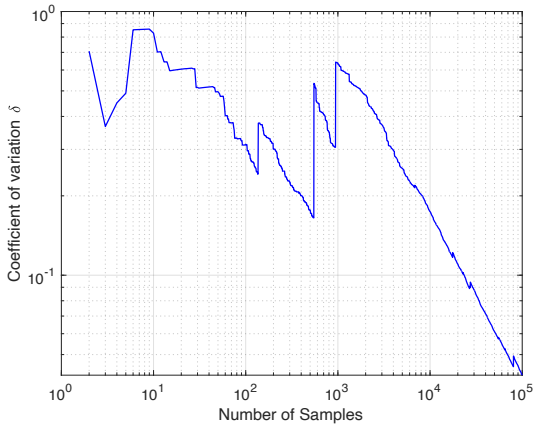

(a) $\nu = 3$

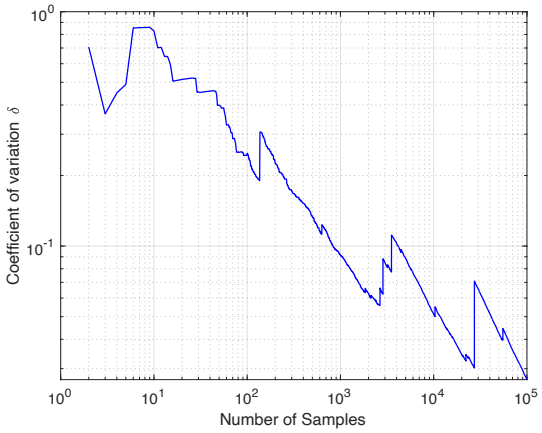

(b) $\nu = 5$

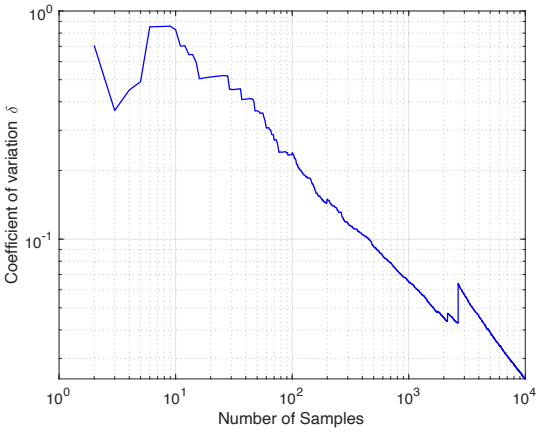

(c) $\nu = 10$

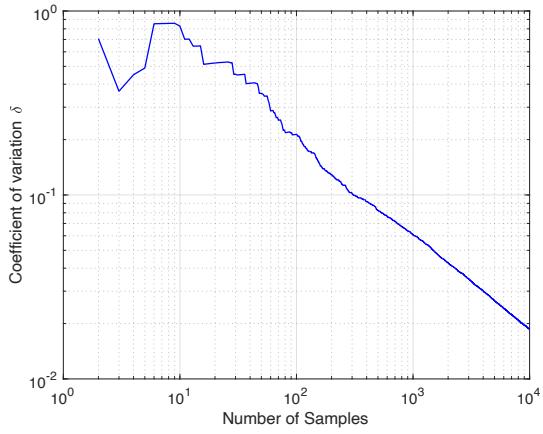

(d) $\nu = 30$

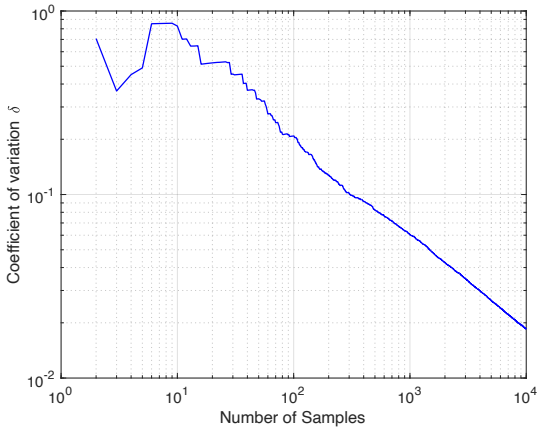

(e) $\nu = 100$

Figure 4-31: Evolution of the coefficient of variation for different values of ν parameter for MDOF system

5 Conclusions

A new method for estimating failure probability has been developed, which is suitable for structural systems subjected to stochastic dynamic loading. The basic procedure of Importance Sampling is modified and tailored to approximate non-Gaussian loadings as Gaussian.

This method begins by approximating the structure's response as Gaussian and then comparing it to the actual non-Gaussian response of the system. Reliability indices for every response of interest are calculated, and reference points (approximated design points) are defined. Based on the calculated reliability indices, weights for every time step are calculated as well. Failure samples are generated firstly in Gaussian space, then transferred to physical space, and used for the calculation of the response of a system. Failure probability of a system is estimated with respect to the specified thresholds for up-crossing and down-crossing. The relationship between characterization parameters, approximation accuracy, and failure probability is illustrated graphically.

This study demonstrates the application of the developed method in three examples involving structures subjected to Student's t-distributed loads. The multi degree of freedom example represents a practical application in machining and is highly related to manufacturing, where the Student's t distribution characterizes the force applied to the system. In this case, Student's t distribution models the cutting force fluctuation that occur during the machining of ceramic matrix composites, arising when the cutting tool interacts with the fiber inclusions. These stochastic cutting force variations are a result of the stochastic distribution of fibers within the material. The proposed method achieves higher efficiency and lower computational effort compared to traditional, general approaches such as Monte Carlo Simulation. It has been investigated that the proposed Importance Sampling Using Reference Points method is suitable and works well for the cases when the Gaussianisation of the original non-Gaussian loading is reasonable, e.g. non-Gaussian loading is not too far away from a Gaussian loading. For the presented examples with a Student's t loading, ISURP does not perform well for small values of ν parameter such as $\nu = 3$ and $\nu = 5$.

However, the proposed Importance Sampling Using Reference Points method has not been compared to the Subset Simulation. Consequently, conclusions regarding its efficiency and accuracy relative to SS cannot be drawn. Additionally, the method presented in this thesis may not be unique, and alternative strategies for generating Gaussian approximations could be explored. It is important to note that this study focuses solely on non-Gaussian white noise. Extending the approach to non-Gaussian colored noise with modulation remains a significant challenge. Future research could investigate the applicability of ISURP to larger and more complex structures.

References

[1] Y. K. Wen, "Reliability and performance-based design," *Structural safety,* vol. 23, no. 4, pp. 407-428, 2001.

[2] M. A. Misraji, M. A. Valdebenito, H. A. Jensen and C. F. Mayorga, "Application of directional importance sampling for estimation of first excursion probabilities of linear structural systems subject to stochastic Gaussian loading," *Mechanical systems and signal processing,* vol. 139, no. 106621, p. 106621, 2020.

[3] S. K. Au and J. L. Beck, "First excursion probabilities for linear systems by very efficient importance sampling," *Probabilistic engineering mechanics,* vol. 16, no. 3, pp. 193-207, 2001.

[4] D. Benasciutti and R. Tovo, "Fatigue life assessment in non-Gaussian random loadings," *International journal of fatigue,* vol. 28, no. 7, pp. 733-746, 2006.

[5] X. Ma and Z. Liu, "Influence of ground motion non-Gaussianity on seismic performance of buildings," *Buildings,* vol. 14, no. 8, p. 2364, 2024.

[6] R. Y. Rubinstein, Simulation and the Monte Carlo method, Wiley, 1981.

[7] J. M. Hammersley and D. C. Handscomb, Monte-Carlo methods, London: Methuen, 1964.

[8] G. I. Schuëller and R. Stix, "A critical appraisal of methods to determine failure probabilities," *Struct Safety,* vol. 4, pp. 293-309, 1987.

[9] M. Shinozuka, "Basic analysis of structural safety," *Journal of structural engineering (New York, N.Y.),* vol. 109, no. 3, pp. 721-740, 1983.

[10] S.-K. Au and J. L. Beck, "Estimation of small failure probabilities in high dimensions by subset simulation," *Probabilistic engineering mechanics,* vol. 16, no. 4, pp. 263-277, 2001.

[11] R. E. Melchers, "Importance sampling in structural systems," vol. 6, no. 1, pp. 3-10, 1989.

[12] M. Hohenbichler and R. Rackwitz, "Improvement of second-order reliability estimates by importance sampling," *Journal of engineering mechanics,* vol. 114, no. 12, pp. 2195-2199, 1988.

[13] C. Papadimitriou, J. L. Beck and L. S. Katafygiotis, "Asymptotic expansions for reliability and moments of uncertain systems," *Journal of engineering mechanics,* vol. 123, no. 12, pp. 1219-1229, 1997.

[14] A. Der Kiureghian and T. Dakessian, "Multiple design points in first and second-order reliability," *Structural safety,* vol. 20, no. 1, pp. 37-49, 1998.

[15] S. K. Au, C. Papadimitriou and J. L. Beck, "Reliability of uncertain dynamical systems with multiple design points," *Structural safety,* vol. 21, no. 2, pp. 113-133, 1999.

[16] C. G. Bucher, "Adaptive sampling — an iterative fast Monte Carlo procedure," *Structural safety,* vol. 5, no. 2, pp. 119-126, 1988.

[17] A. Karamchandani, P. Bjerager and C. A. Cornell, "Adaptive importance sampling," in *Proceedings of the Fifth ICOSSAR*, San Francisco, 1989.

[18] G. L. Ang, A. H. Ang and -S. Tang, "Optimal importance sampling density estimator," *Journal of Engineering Mechanics-asce,* vol. 118, pp. 1146-1163, 1992.

[19] S. K. Au and J. L. Beck, "A new adaptive importance sampling scheme for reliability calculations," *Structural safety,* vol. 21, no. 2, pp. 135-158, 1999.

[20] G. I. Schuëller, H. J. Pradlwarter and M. D. Pandey, "Methods for reliability assessment of nonlinear systems under stochastic dynamic loading - a review," in *Proceedings of EURODYN'93*, 1993.

[21] S. K. Au and J. L. Beck, "Important sampling in high dimensions," *Structural safety,* vol. 25, no. 2, pp. 139-163, 2003.

[22] L. S. Katafygiotis and K. M. Zuev, "Estimation of small failure probabilities in high dimensions by adaptive linked importance sampling," *COMPDYN,* 2007.

[23] L. Katafygiotis and S. H. Cheung, "Domain decomposition method for calculating the failure probability of linear dynamic systems subjected to Gaussian stochastic loads," *Journal of engineering mechanics,* vol. 132, no. 5, pp. 475-486, 2006.

[24] P. Bjerager, "Probability integration by directional simulation," *Journal of engineering mechanics,* vol. 114, no. 8, pp. 1285-1302, 1988.

[25] O. Ditlevsen, P. Bjerager, R. Olesen and A. M. Hasofer, "Directional simulation in Gaussian processes," *Probabilistic engineering mechanics,* vol. 3, no. 4, pp. 207-217, 1988.

[26] S. K. Au and Y. Wang, Engineering Risk Assessment with Subset Simulation, John Wiley & Sons, 2014.

[27] L. S. Katafygiotis and S. H. Cheung, "Application of spherical subset simulation method and auxiliary domain method on a benchmark reliability study," *Structural safety,* vol. 29, no. 3, pp. 194-207, 2007.

[28] G. S. Fishman, Monte Carlo: Concepts, Algorithms, and Applications, NewYork: Springer, 1996.

[29] X.-Y. Zhang, M. A. Misraji, M. A. Valdebenito and M. G. R. Faes, "Directional Importance Sampling for Dynamic Reliability of Linear Structures under Non-Gaussian White Noise Excitation," *Mechanical Systems and Signal Processing,* 2024.

[30] K.-J. Bathe, Finite element procedures, Prentice Hall Englewood Cliffs, NJ, 1996.

[31] H. A. Jensen, "Structural optimization of linear dynamical systems under stochastic excitation: a moving reliability database approach," *Computer methods in applied mechanics and engineering,* vol. 194, no. 12-16, pp. 1757-1778, 2005.

[32] "Uml.edu," [Online]. Available: https://ws-website-dco-prod-lb-01.uml.edu/docs/second-impulse_tcm18-190094.pdf. [Accessed 17 12 2024].

[33] R. L. Burden, Numerical analysis, Brooks/Cole Cengage Learning, 2011.

[34] "Introduction to the Problem of Structural Reliability and Use of the Monte Carlo Simulation Technique," TU Dortmund, Chair for Reliability Engineering, Tutorial notes, 2024.

[35] "Importance Sampling – Part 1," TU Dortmund, Chair for Reliability Engineering, Tutorial notes, 2024.

[36] "Importance Sampling – Part 2," TU Dortmund, Chair for Reliability Engineering, Tutorial notes, 2024.

[37] H. Kamper, "Hidden Markov models," [Online]. Available: https://www.kamperh.com/nlp817/notes/05_hmm_notes.pdf. [Accessed 17 12 2024].

[38] "Simulation Considering Conditional Distributions," TU Dortmund, Chair for Reliability Engineering, Tutorial notes, 2024.

[39] A. Kiureghian, "The geometry of random vibrations and solutions by FORM and SORM," *Probabilistic Engineering Mechanics,* vol. 15, no. 1, pp. 81-90, 2000.

[40] "Efficient Importance Sampling," TU Dortmund, Chair for Reliability Engineering, Tutorial notes, 2024.

[41] M. Taboga, "Student's t distribution," Lectures on probability theory and mathematical statistics, Kindle Direct Publishing, Online appendix, https://www.statlect.com/probability-distributions/student-t-distribution, 2021.

[42] A. Rudolph, J. Krois and K. Hartmann, "Statistics and Geodata Analysis using Python (SOGA-Py)," Department of Earth Sciences, Freie Universität Berlin, 2023.

[43] H. W. Park, Y. B. Park and S. Y. Liang, "Multi-procedure design optimization and analysis of mesoscale machine tools," *The international journal of advanced manufacturing technology,* vol. 56, no. 1-4, pp. 1-12, 2011.

[44] X. Zhang, T. Yu and J. Zhao, "An analytical approach on stochastic model for cutting force prediction in milling ceramic matrix composites," *International journal of mechanical sciences,* vol. 168, no. 105314, p. 105314, 2020.

[45] J. Mei, O. G. Diaz and D. A. Axinte, "Modelling the unidirectional fibre composite milling force oscillations through capturing the influence of the stochastic fibre distributions," *Composite structures,* vol. 226, no. 111188, p. 111188, 2019.

[46] Y. Liu, Z. Xiong and Z. Liu, "Stochastic cutting force modeling and prediction in machining," *Journal of manufacturing science and engineering,* vol. 142, no. 12, 2020.

[47] G. Fodor, H. T. Sykora and D. Bachrathy, "Stochastic modeling of the cutting force in turning processes," *The international journal of advanced manufacturing technology,* vol. 111, no. 1-2, pp. 213-226, 2020.

Affidavit

Eidesstattliche Versicherung

(Affidavit)

Besedin, Maksym
Name, Vorname
(surname, first name)

243358
Matrikelnummer
(student ID number)

☐ Bachelorarbeit
(Bachelor's thesis)

■ Masterarbeit
(Master's thesis)

Titel
(Title)

Development of a Method for Assessing the Reliability of Machines Operating Under Stochastic Dynamic Loading

Ich versichere hiermit an Eides statt, dass ich die vorliegende Abschlussarbeit mit dem oben genannten Titel selbstständig und ohne unzulässige fremde Hilfe erbracht habe. Ich habe keine anderen als die angegebenen Quellen und Hilfsmittel benutzt sowie wörtliche und sinngemäße Zitate kenntlich gemacht. Die Arbeit hat in gleicher oder ähnlicher Form noch keiner Prüfungsbehörde vorgelegen.

I declare in lieu of oath that I have completed the present thesis with the above-mentioned title independently and without any unauthorized assistance. I have not used any other sources or aids than the ones listed and have documented quotations and paraphrases as such. The thesis in its current or similar version has not been submitted to an auditing institution before.

Dortmund, 13.01.2025
Ort, Datum
(place, date)

Unterschrift
(signature)

Belehrung:
Wer vorsätzlich gegen eine die Täuschung über Prüfungsleistungen betreffende Regelung einer Hochschulprüfungsordnung verstößt, handelt ordnungswidrig. Die Ordnungswidrigkeit kann mit einer Geldbuße von bis zu 50.000,00 € geahndet werden. Zuständige Verwaltungsbehörde für die Verfolgung und Ahndung von Ordnungswidrigkeiten ist der Kanzler/die Kanzlerin der Technischen Universität Dortmund. Im Falle eines mehrfachen oder sonstigen schwerwiegenden Täuschungsversuches kann der Prüfling zudem exmatrikuliert werden. (§ 63 Abs. 5 Hochschulgesetz - HG -).

Die Abgabe einer falschen Versicherung an Eides statt wird mit Freiheitsstrafe bis zu 3 Jahren oder mit Geldstrafe bestraft.

Die Technische Universität Dortmund wird ggf. elektronische Vergleichswerkzeuge (wie z.B. die Software „turnitin") zur Überprüfung von Ordnungswidrigkeiten in Prüfungsverfahren nutzen.

Die oben stehende Belehrung habe ich zur Kenntnis genommen:

Official notification:
Any person who intentionally breaches any regulation of university examination regulations relating to deception in examination performance is acting improperly. This offense can be punished with a fine of up to EUR 50,000.00. The competent administrative authority for the pursuit and prosecution of offenses of this type is the Chancellor of TU Dortmund University. In the case of multiple or other serious attempts at deception, the examinee can also be unenrolled, Section 63 (5) North Rhine-Westphalia Higher Education Act (*Hochschulgesetz, HG*).

The submission of a false affidavit will be punished with a prison sentence of up to three years or a fine.

As may be necessary, TU Dortmund University will make use of electronic plagiarism-prevention tools (e.g. the "turnitin" service) in order to monitor violations during the examination procedures.

I have taken note of the above official notification:*

Dortmund, 13.01.2025
Ort, Datum
(place, date)

Unterschrift
(signature)

***Please be aware that solely the German version of the affidavit ("Eidesstattliche Versicherung") for the Bachelor's/ Master's thesis is the official and legally binding version.**